Phantom Digital Subscriber Loops

Measurement, Identification and Capacity Assessments

{ Draft }

Narendra Kumar Saini,
Marc Moonen

Abstract

In this document we carry out measurements on a Cat5e, 0.5mm UTP 4-pair copper cable to identify the capacity gains of a Phantom DSL over a traditional normal DSL. Frequency domain identification of the channels are carried out and capacity comparisons between normal and equivalent phantom DSL were drawn. Gigabits on a Phantom DSL is discussed and a relationship between Phantom and normal channel is established. A power sum model for self-FEXT is also suggested. In the end future course of action is also suggested based on the out come of these measurements and capacity assessments.

Abbreviation

The following acronyms and abbreviations are used in the report

10MDSL	10 Mbps DSL
100MDSL	100 Mbps DSL
ADSL	Asymmetric Digital Subscriber Loop
ANSI	American National Standard Institute
AWG	American Wire Gauge
AWGN	Additive White Gaussian Noise
CO	Central Office
BC	Broadcast Channel
CPE	Customer Premise Equipment
CSA	Carrier Servicing Area
DFE	Decision Feedback Equalizer
DMT	Discrete Multi-tone
DSL	Digital Subscriber Loop
DSLAM	Digital Subscriber Loop Access Multiplexer
DSM	Dynamic Spectrum Management
DUT	Device under test
dB	tenth of a Bell, deciBell
dBm	deciBell with reference to 1mW of power
ETSI	European Telecommunication Standard Institute
FDD	Frequency Division Duplex
FEXT	Far End Crosstalk
GDFE	Generalized Decision Feedback Equalizer
GDSL	Gigabit Digital Subscriber Loop
G/K/M bps	Giga/Mega/Kilo -bits-per-second
iid	Independently and Identically Distributed
kft	Length of cable in kilofeet
LAN	Local Area Network
M/KHz	Frequency in mega/kilo Hz
MAC	Multi Access Channel
MDSL	Multi-line DSL

MIMO	Multi-input-multi-output
NEXT	Near End Crosstalk
PSD	Power Spectral Density
PSFEXT	Power Sum FEXT
RLCG	Resistance, Inductance, Capacitance and Conductance of a DSL line
SNR	Signal-to-noise-ratio
T1A	Telecommunications Industry Association
VDSL	Very-high Data Rate DSL

Table of Contents

List of Figures

List of Tables

Chapter 1

Introduction

The chapter begins with the definition of Phantom Mode DSL and its comparison with the Normal Mode DSL. The purpose of the measurement is stated and organization of the report is provided towards the end.

1.1 Introduction

The telephones were first used for the transmission of voice data was performed with a single wire [1]. The reference ground to the wireline system was provided at the customer premise. In this case, only one wire per customer line was used.

The communication system had a big drawback of the reference ground. In summers, it was usual that the reference ground (wire) at customer premise is dried up and did not provide sufficient grounding. The substantial loss in the quality of service was noted in dry weather. At a later stage, a ground wire was also provided along with the wire used as communication channel to provide a good ground reference to the communication system both at customer premise as well as the central office. It facilitated the robust quality of service against the environmental changes. For every single connection a reference ground was provided i.e. for n connections, $2n$ wires were used.

Due to several lines running in parallel, crosstalk between the lines started appearing as a degradation to the quality of service for longer lines. As the number of telephone lines increased, there were concerns about feasible solutions of the crosstalk. By that time, Maxwell's equations of electrodynamics were understood well. As an intuition (and a fact for physicist), it became clear that twisting of the wires would cancel the electromagnetic interference to an acceptable level. The twisted wire pairs were introduced by Bell company to the telephone market. It substantially decreased the crosstalk levels and proved to be a considerable improvement in the quality of service in telephone sector.

DSL technology was introduced to convert these traditional voice band channels to wide-band information bearing channels. Its variant ADSL is a widely popular technology and further work is going on the next generation Very-high-data-rate DSL (VDSL) within the wireline community. In our discussions now on, we will refer this as Normal mode DSL technology, unless otherwise specified.

1.2 Phantom Mode

The Phantom mode DSL picks up the idea from early days of telephone line deployment. Instead of providing a reference ground to every single wire separately, it suggests to provide only one reference wire to a single customer premise. It can as well be a residential colony or a small business center, however it is obvious that the crosstalk in such a system will be huge and proper techniques have to be introduced to counter this crosstalk.

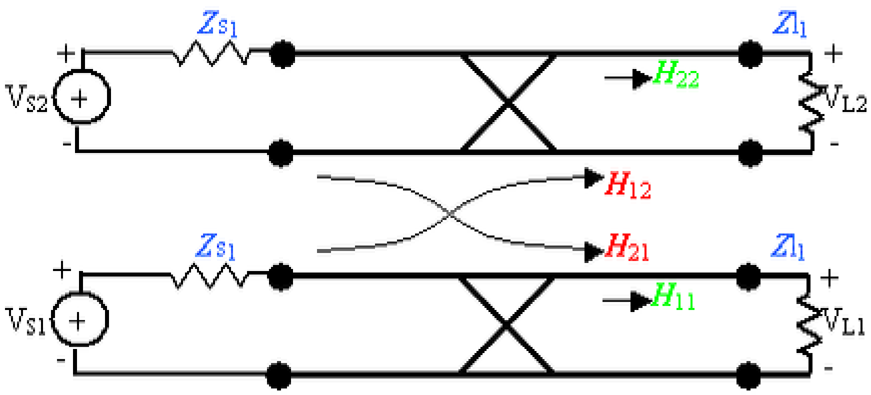

Figure 1.1: Normal Mode DSL (two active loop-pairs)

Only one reference ground translates into more number of parallel data channels availability with the same number of pairs. If there are n telephone lines to the customer premise, in all $2n-1$ data channels should be available for the data transfer above voice band. It is opposite to that of only n data channels in the previous (existing) schemes. A direct benefit of $n-1$ channels could be translated into a higher available data rates at DSL distances.

The phantom mode DSL is explained graphically through Figure 1.2. A comparison with normal mode DSL is also provided with Figure 1.1. For example, consider two twisted wire pairs are available to a customer premise. One of the pair is being used in a DSL loop and the other is used only for voice band communications (telephone). More than one telephone lines to a single customer premise are not very uncommon in European and North American continent.

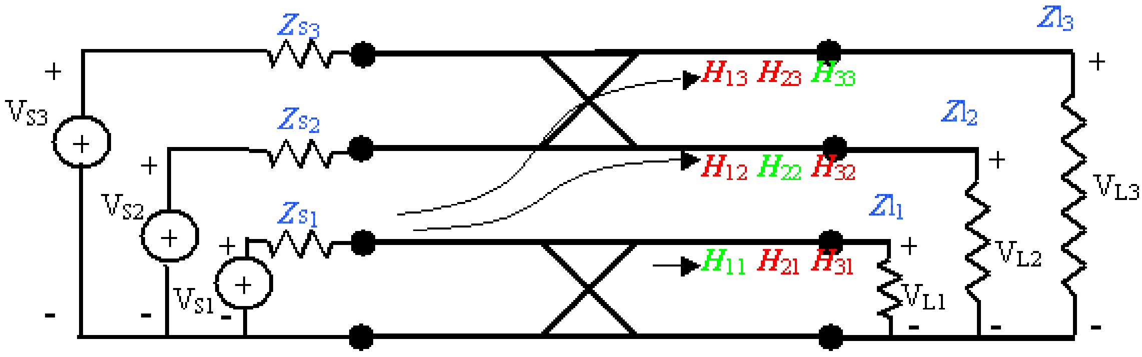

Figure 1.2: Phantom Mode (three active data-wires)

In Figure 1.1 and Figure 1.2, a wire-pair with a cross designates a twisted pair. For normal mode DSL, Figure 1.1. applies where each twisted pair is assumed to be one stand-alone channel in practice. It is assumed that both the loops are being used as DSL channel. Figure 1.2 depicts a Phantom mode of DSL loop where two twisted pairs are sharing a single ground (reference) and hence we have an extra data channel with the same number of twisted pairs. If n is the number of twisted pairs involved in a Phantom mode then the number of parallel channels so obtained will be $2n - 1$.

In more general terms, a Phantom mode (or sometime referred as multi-line DSL [5] [2]) can have a $2n - 1$ data wires with any one arbitrarily chosen reference wire from the bundle (or cable).

1.3 Purpose

The motivation behind the measurements and the capacity assessments was to have an idea of gains of a Phantom mode DSL connection over a Normal mode connection. It is obvious that in such a scenario the crosstalk is inherent to the system and efficient use of Phantom mode DSL will mostly depend on the crosstalk mitigation techniques.

In magnitude, the near-end-crosstalk (NEXT) is much larger than the far-end-crosstalk (FEXT). In discrete-multitone (DMT) systems NEXT is controlled via frequency division duplexing (FDD). The FEXT remains the main source of crosstalk in the long lines. This degrades the signal-to-noise ratio (SNR) at higher frequencies and limits the effective loop length for considerable data rates. FEXT mitigation schemes would gain importance in future so as to increase the data rates on the existing DSL loops as well as in terms of loop-length. Fig. 1.1 and 1.2 assumes that the NEXT is not present (also for overlapping upstream and downstream

DSLs using echo-cancelation schemes) and FEXT is the only source of crosstalk noise. Hereafter we will assume FEXT crosstalk noise to be the dominant source of noise in DSL. The FEXT transfer functions from one line to the rest of the data-wires in the system are shown as $\mathbf{H}_{i,j}(f)$, where $i, j = 0, \ldots, n$ for normal mode and $i, j = 0, \ldots, 2n-1$ for phantom mode, are data-wire in the system (Normal or Phantom) under consideration. For $i = j$, it is the direct transfer function of the i^{th} data-wire. Frequency notation f is omitted for the simplicity.

$$\begin{bmatrix} \mathbf{H}_{11} & \mathbf{H}_{12} & \ldots & \mathbf{H}_{1n} \\ \mathbf{H}_{21} & \ddots & & \vdots \\ \vdots & & \ddots & \vdots \\ \vdots & & & \vdots \\ \mathbf{H}_{n1} & \ldots & & \mathbf{H}_{nn} \end{bmatrix} \tag{1.1}$$

It is assumed that as the loop-unbundling will eventually take place and service provider would be inclined to use the packet based services with single DSLAM at the CO and coordination among different DSL loops should be possible [1].

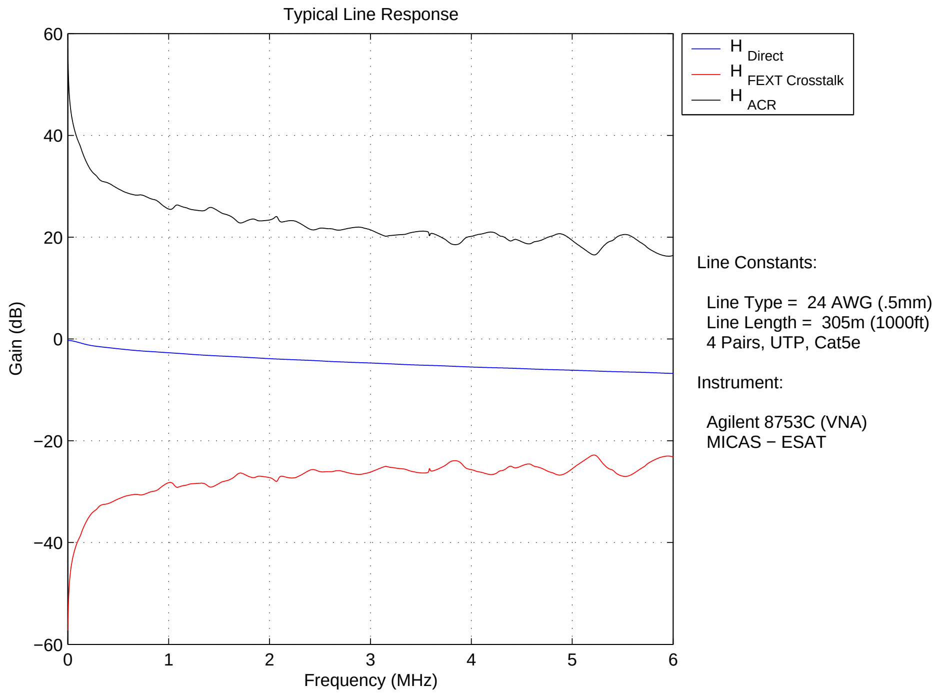

Figure 1.3: Typical response and ACR of a Normal channel)

Considering Phantom mode as a Multi-Input-Multi-Output (MIMO) system can lead to the reduction or total mitigation to the FEXT crosstalk. Vectored transmission [10] is seen as a solution to the crosstalk in such a scenario where the coordination among the wire is possible at the CO. In this case, a Phantom channel can be considered as a MIMO system at each tone, considering Frequency Division Duplex (FDD). The downstream channel is therefore con-

sidered as broadcast channel (BC) and the upstream channel can be modeled as a multiacess channel (MAC).
The multiline and phantom DSL are being seen as the DSL techniques of time to come. It has received substantial attention in the recent past. It is obvious from the proposals of 10MDSL and MMDSL. Multiline copper pair transmission has also been referred in the recent draft of Ethernet in First Mile (EFM) task force [8], constituted by IEEE [12]. The final draft of the EFM standards is available. The quest of high data rate on twisted pairs would eventually lead to the evolution of multiline communication theory and practices.

1.4 Organization of the report

The report is organized in four parts. This chapter gives an introduction to the Phantom Mode and compared with the Normal Mode DSL. The purpose of the work carried out so far is also stated in the second section.

Chapter 2 is dedicated to the measurements made during the work. It contains the brief introduction to the basic transmission line and a discussion on multi-line model is provided. For simplicity the discussion is limited to the two-wire pairs (i.e. three data wire and a reference wire), but can be generalized to three-pair wire system and further.

Chapter on Channel Identification gives a brief overview of Identification process and frequency domain approach to the system identification. The subject is discussed only in the reference of the model identification for the direct and crosstalk channel measurements discussed in Chapter 3.

As mentioned previously, the main purpose of the measurements carried out during this work was to identify the gains obtained from a Phantom mode DSL then that of the Normal mode DSL system. These gains are discussed in the chapter of Capacity calculations. A brief overview of vectored transmission is provided. Vectored transmission is considered to be very effective wherever coordination is possible. It is assumed that for every user the transmitters for downstream and the receivers for upstreams are co-located at CO and hence the coordination can be achieved. A comparison is drawn between the achievable capacities on Phantom mode and Normal mode DSL's before and after the crosstalk mitigation, assuming that the crosstalk is completely removed through vectored transmission techniques. Towards the end Gigabits on Phantom DSL is discussed assuming that the crosstalk can be completely mitigated.

The relations between Phantom channel and the normal channel matrices is also discussed. it is interesting to see that the basic physics (electromagnetics) helps in deeper understanding of the crosstalk couplings of a phantom channel and relates well to the normal channel. Power sum self-FEXT crosstalk model is discussed and explained in short.

In the end conclusion of the experiments carried out and their possible impact on the data rate and capacities is drawn. Future work in this regards is also been highlighted towards the end.

Chapter 2

Measurements

As described in previous chapter, crosstalk noise is inherent to Phantom Mode DSL. It is clear that the electromagnetic interference in parallel Phantom channels will be more then two independent DSL loops as described in Figure 1.1 and Figure 1.2. Moreover crosstalk in the two wires twisted in a single pair will be much higher when compared to the crosstalk between a wire paired with the reference (ground) and the rest or if the two wire belongs to two different phantom pairs (if more then two twisted pairs are used). Before starting a small review of basics of transmission line is given.

2.1 Transmission lines

In this section only a brief review is provided, for details please look at the various texts, for example [15], [16] [14] and the references there in.

A transmission line can be modeled as a composition of infinitesimal sections of lumped circuits of length Δx (dx), as shown in Figure 2.1 . The system of two transmission lines can be translated into the following coupled equations,

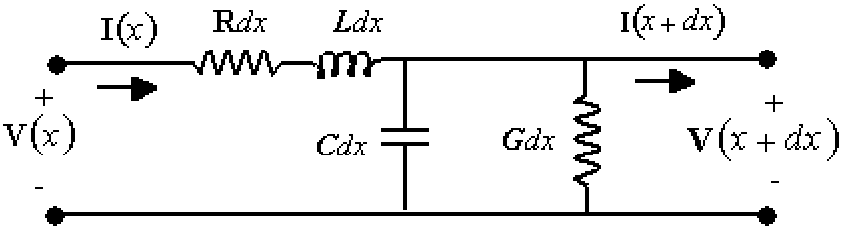

Figure 2.1: Incremental Model for transmission line (2-conductors)

$$\frac{\partial}{\partial x}v(x,t) = -Ri(x,t) - L\frac{\partial}{\partial x}i(x,t), \tag{2.1a}$$

$$\frac{\partial}{\partial x}i(x,t) = -Gv(x,t) - C\frac{\partial}{\partial x}v(x,t) \tag{2.1b}$$

Where, R is the resistance, L the inductance, C the capacitance and G is the conductance of this infinitesimal section. The system of these coupled equation can be solved by second-order differential equations. It can be shown that the solution of these two equation leads to the sum of two waves traveling in opposite directions in the transmission line. The resulting equations are,

$$V(x) = {V_0}^+e^{-\gamma x} + {V_0}^-e^{+\gamma x} \tag{2.2a}$$

$$I(x) = {I_0}^+e^{-\gamma x} + {I_0}^-e^{+\gamma x} \tag{2.2b}$$

where,

$$\begin{aligned}\gamma &= \alpha + j\beta \\ &= \sqrt{(R + j\omega L)(G + j\omega C)}\end{aligned} \tag{2.3}$$

Where γ is the propagation constant of the transmission line, α is the attenuation constant, and β is the phase constant. The forward-traveling voltage and current are related by the characteristic impedance of the transmission line, namely Z_0. The relation is,

$$Z_0 = \frac{{V_0}^+}{{I_0}^+} = \frac{{V_0}^-}{{I_0}^-} = \sqrt{\frac{R + j\omega L}{G + j\omega C}} \tag{2.4}$$

For practical purposes, characteristic impedance Z_0 is calculated via short circuited impedance Z_{sc} and open circuited impedance Z_{oc}. The propagation constant γ can also be calculated with Z_{sc} and Z_{oc} using the following relationship,

$$Z_0 = \sqrt{Z_{sc}.Z_{oc}} \tag{2.5a}$$

$$\gamma = \frac{1}{d}\tanh^{-1}\sqrt{\frac{Z_{sc}}{Z_{oc}}} \tag{2.5b}$$

As stated before resistance(R), inductance(L), capacitance(C) and conductance(G) are the primary cable parameters of a transmission line and are commonly identified as RLCG parameters. The secondary parameters are the characteristic impedance Z_0 and Propagation constant γ. It is shown that these parameters are related as,

$$\mathbf{R} = \Re\{\gamma . Z_0\} \tag{2.6a}$$

$$\mathbf{L} = \frac{1}{\omega}\Im\{\gamma . Z_0\} \tag{2.6b}$$

$$\mathbf{C} = \frac{1}{\omega}\Im\{Z_0{}^{-1}.\gamma\} \tag{2.6c}$$

$$\mathbf{G} = \Re\{Z_0{}^{-1}.\gamma\} \tag{2.6d}$$

It must be emphasized that in case of multi-port network, these parameters would take the form of matrices. Such a system can therefore be modeled as a MIMO system which is briefly described in the following section.

2.1.1 Multi-line Model

As growing interest in the DSL technology ([5], [2] and Phantom DSL), a multi-line approach for the higher data rate and long loop reach is being studied by research community. There are examples of LAN where MIMO techniques are already in use to combat the crosstalks among the data-carrying wires [9]. 100 Mbps are already being deliverd on a LAN connections while standards for 1 Gpbs and 10 Gpbs data rates are already in the pipeline. While these data rates are possible on the copper network, interests are growing in the DSL community to use more then one wire for the data-transmission and the study of feasibility of MIMO communication in DSL [8].

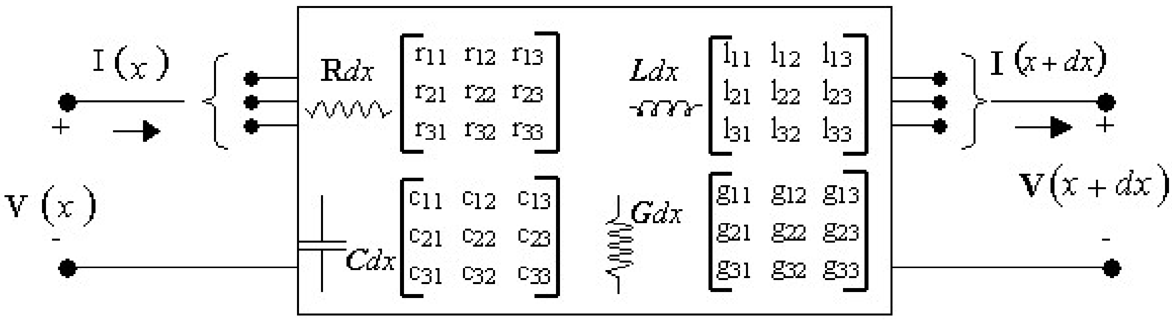

Figure 2.2: Phantom Mode (three active data-wires)

As described in the previous section, when a multiline model of transmission line is considered, the equation described in the last section still applies but the parameters take the form of matrices. The components of RLCG matrix in themselves are matrices. These matrices do not only convey information for the direct channel RLCG parameters of a line but also reflects their inter-dependance when used in a multi-line mode. The new entries to the RLCG matrices gives an idea of the parameters for the crosstalk within the lines of the multi-line system so evolved. A model for possible scenario of the RLCG matrices in a multi-line model is depicted in Figure 2.2 .

According to the multi-line model, as in Figure 2.2,

$$V(x+dx) = \begin{bmatrix} v_{11}(x+dx) & v_{12}(x+dx) & v_{13}(x+dx) \\ v_{21}(x+dx) & v_{22}(x+dx) & v_{23}(x+dx) \\ v_{31}(x+dx) & v_{32}(x+dx) & v_{33}(x+dx) \end{bmatrix} \tag{2.7}$$

where the voltage $v_{i,j}(x + dx)$ for $i \neq j$, is due to the electromagnetic coupling of the lines. The voltage appeared on terminal 1 is the sum of the voltages due to the direct line and the crosstalk due to the other line in Phantom, assuming that the crosstalk from other lines of the bundle not in Phantom, are negligible. It is a realistic situation since the crosstalk within Phantom system is in itself very large compared to the crosstalk appearing due to the lines in in Phantom.

Using similar definitions for the characteristic impedance Z_0 and the reflection coefficient γ, they will also take the form of matrices as the following,

$$\begin{aligned} Z_0(j,k) &= \sqrt{\frac{R(j,k) + j\omega L(j,k)}{G(j,k) + j\omega C(j,k)}} \\ &= \sqrt{Z_{sc}(j,k) \cdot Z_{oc}(j,k)} \\ \gamma(j,k) &= \frac{1}{d_{jk}} \tanh^{-1} \sqrt{\frac{Z_{sc}(j,k)}{Z_{oc}(j,k)}} \end{aligned} \tag{2.8}$$

The transfer function matrix can now be formed from all the information at hand. The individual voltage transfer functions, both for direct and for the crosstalks, can be deduced using Z_0 and γ matrices as the following,

$$V_{multiline}(\text{ or } H_{multiline}) = \begin{bmatrix} \frac{v_{11}^+}{v_{11}^-} & \frac{v_{12}^+}{v_{11}^-} & \frac{v_{13}^+}{v_{11}^-} \\ \frac{v_{21}^+}{v_{22}^-} & \frac{v_{22}^+}{v_{22}^-} & \frac{v_{23}^+}{v_{22}^-} \\ \frac{v_{31}^+}{v_{33}^-} & \frac{v_{32}^+}{v_{33}^-} & \frac{v_{33}^+}{v_{33}^-} \end{bmatrix} = \begin{bmatrix} H_{11} & H_{12} & H_{13} \\ H_{21} & H_{22} & H_{23} \\ H_{31} & H_{32} & H_{33} \end{bmatrix} \tag{2.9}$$

It is obvious that $H_{j,j} > H_{j,k} \quad \forall j \neq k$. It is direct indication of the diagonal dominance in the multi-line model. The subject is not treated much in detail in this report. A classical treatment of the subject along with theoretical background of multi-line modeling for DSL are covered in the recent works [3], [4] and the references therein.

We draw an important conclusions from multiline modelling, **Characteristic Impedance**: The characteristic impedance of every combination of line is different, depending on its physical distance d_{jk} from the other wire in consideration and reflection coefficient $\gamma(j,k)$. For maximum power transfer, the characteristic impedance of all these pairs should be matched prior to the measurement of any multiline transfer function.

2.1.2 S-parameter and transmission lines

A rich theory of two port and multi-port measurements for the transmission line exists. In various texts details of Z-parameters, Y-parameters, S-parameters and H-parameters can be found. Another more popular approach is to use ABCD parameters [14] for the transmission line measurements. Once any of the parameter-set is obtained, other parameter set can easily be obtained.

Out of these different set of parameters, S-parameters are easily measured and most of the instruments, e.g. vector network analyzers (VNA), rely on S-parameter measurements. A classical treatment is provided in [13]. We skip the introduction of S-parameters in the report and refer to [13] and [14] for further interest.

2.2 Measurements

The whole measurement procedure of phantom and normal mode DSL channel was accomplished in the following two steps,

1. Measurements of the characteristic impedance in different pairs
2. Channel response measurements

As discussed in the previous section, for the maximum power transfer the network should be matched to its characteristic impedance at every node. It is, therefore, characteristic impedance matrix $\mathbf{Z}_0$ is measured prior to the measurement of Phantom channel.

The direct and crosstalk channels are than identified. The identification process of the channels is discussed in the next chapter. Before starting measurements a small description of experimental setup and other necessary information is provided.

2.2.1 Experimental Setup

The impedances measurements were performed in MICAS-lab using vector network analyzer HP-8753C [17]. A vector network analyzer rely on S-parameter test procedure. A typical vector network analyzer set up is shown in Figure 2.3. The experiment setup consists of the following equipments,

- Vector Network Analyzer (VNA),
- Device Under Test (DUT) - 24 AWG copper wire, 305 meters,
- Proper connectors to connect the cable to VNA, so as to reduce the reflection at the interconnections to a minimum,
- Storage disk for measurement data (if the instrument is not directly connected to a computer).

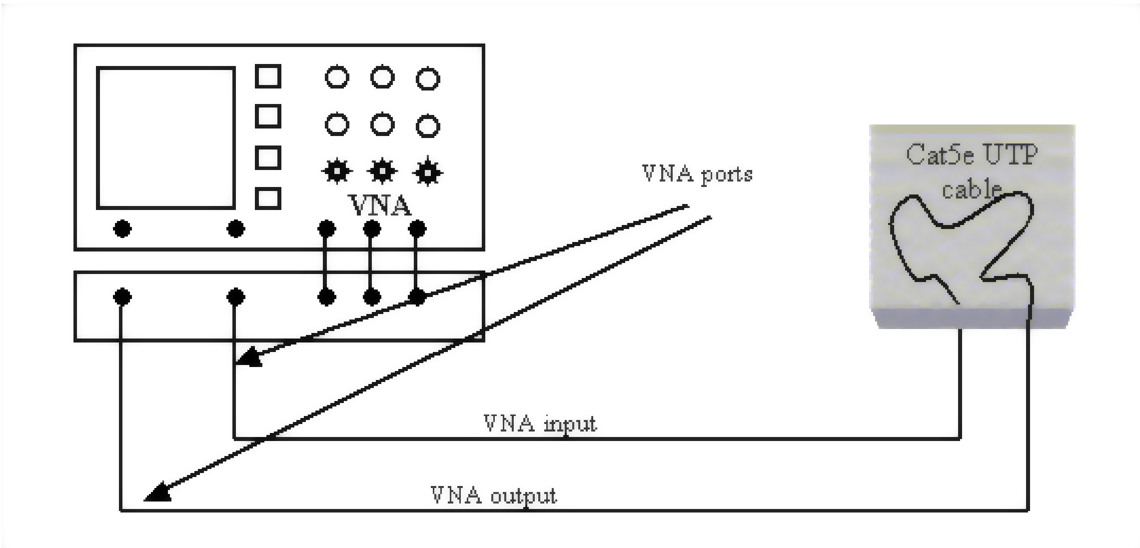

Figure 2.3: Vector Network Analyzer Set-up

The channel measurements were performed in RF-Laboratory [18] using two port methodology for each individual transfer function of the DSL channel matrix. Vector network analyzer of Agilent 8753ES was used for channel measurement.

2.2.2 Measurements of the characteristic impedances

As described in the previous sections the transmission line should be terminated in its characteristic impedance for the maximum power transfer. It is intuitive that with the change in the geometry of wires (in Phantom Mode they are geometrically distributed within the cable),

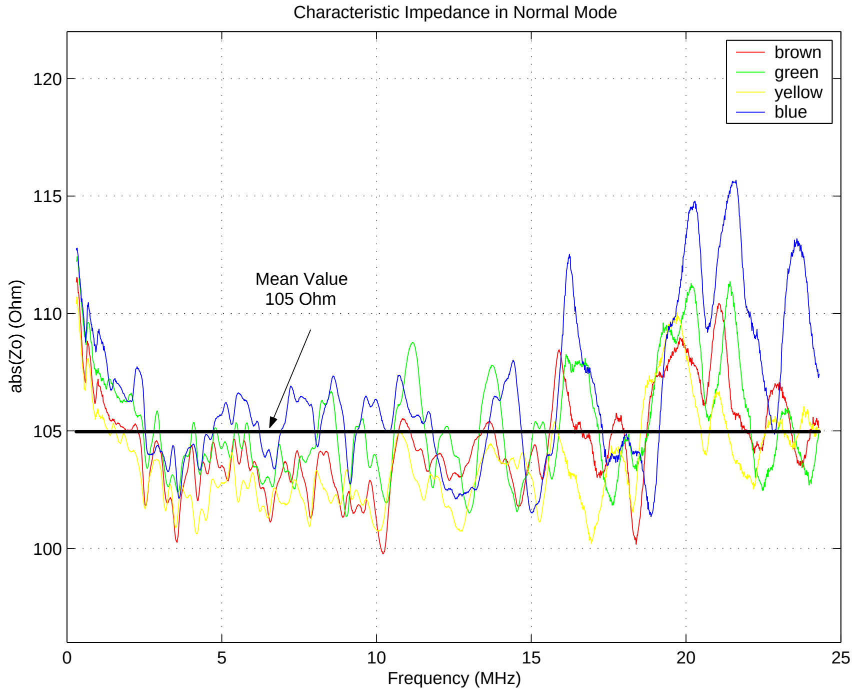

Figure 2.4: Characteristic Impedances of twisted pairs in normal mode.

the characteristic impedance of different combination with the reference wire also changes. In fact the RLCG parameter should be different for every different combination of the wire pairs and therefore, the need of a multi-line model arises (see Sec. 2.1.1).

For the measurement of the characteristic impedance, a simple method of short and open channel was implied. The short circuited impedance Z_{sc} and open circuited impedance Z_{oc} were calculated from S-parameter set. The characteristic impedance Z_0 of the line under consideration can therefore be given as,

$$Z_0 = \sqrt{Z_{sc}.Z_{oc}} \tag{2.10}$$

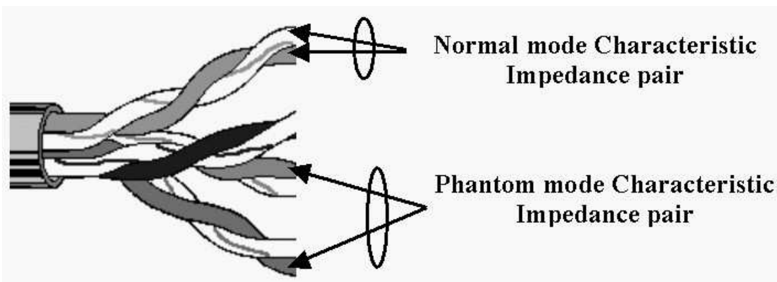

Figure 2.5: Explanation of twist density and initial phase difference in Phantom DSL

Since Z_{sc} and Z_{oc} are frequency dependent, so is Z_0. The characteristic impedances of normal mode channel are shown in Figure 2.4.

Note that the normal mode characteristic impedances are close to 100 Ohms within 5 – 10% due to imperfection of the cable. Notice also that all the pairs have their characteristic impedance behaviour similar to each other. This is indicative that the characteristic impedance changes across the cable for varying frequency are structural.

Phantom mode characteristic impedances in Figure 2.6 are found to change drastically from their normal mode values. As shown in Figure 2.5, the geometrical and twist density plays an important role in determining these characteristic impedances in Phantom mode.

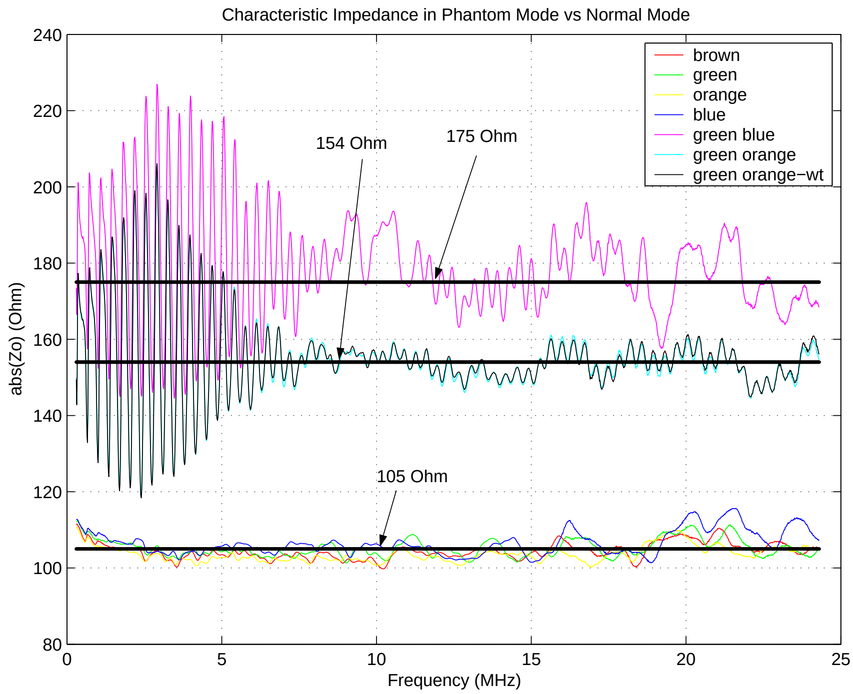

Figure 2.6: Characteristic Impedances in case of a Phantom compared with normal DSL Characteristic impedances.

The characteristic impedances of green and blue (magenta), green and yellow (cyan) and green and yellow-white wires have been shown in the graph. It is clearly seen that yellow and yellow-white (same twist density) have more or less same (cyan and black) characteristic impedances while that with blue is much higher. An approximation of these values can be accepted while approximating them by a resistance throughout the frequency range. Only a few measurements of $Z_0(j,k), \forall j,k = 1,\ldots,n$ are sufficient as the DUT is passive in nature and characteristic impedance matrix will be symmetric. Also as the density of twist per unit length of a pair is same for both wires of that pair, both will share similar characteristic impedances with any other wire in the cable. Note that green is used as the base pair whose other wire, green-wt is used as a ground reference for phantom connections throughout the measurement process.

2.2.3 Measurement of Channel response

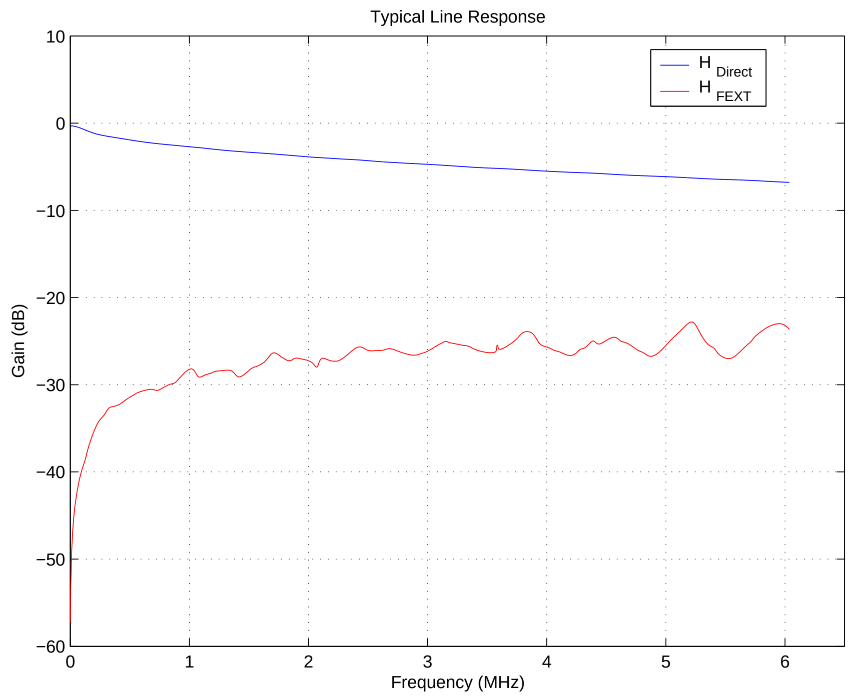

Figure 2.7: Magnitude response of a DSL (normal) channel

The vector network analyzer 8753ES (RF-Lab, IMEC) was used for direct and crosstalk channel measurements. A multiport test system hardware, N4414A was also used for multi-port measurement in differential mode. It is assumed that the crosstalk on a Phantom mode DSL data wire is the power sum of the individual crosstalks due to all other data wire of the Phantom mode DSL system. For the ease of concept, we consider only 2 twisted pairs, which is equivalent to 3 data wires in Phantom mode, to illustrate the measurement process. Later the results of 3 twisted pairs are also shown.

It is important to terminate all the wires in Phantom in their characteristic impedances. As explained in the previous sections, the termination in the characteristic impedance helps in reducing the reflections from the DUT ends.

The Normal mode channel is shown in Figure 2.7. The twisted pairs in Phantom mode are terminated at their characteristic impedances with the ground, and the measurements of crosstalk were made on each wire. The Phantom channel measurement are shown in Figure 2.8. At the time of individual crosstalk and channel measurements, all wires are terminated

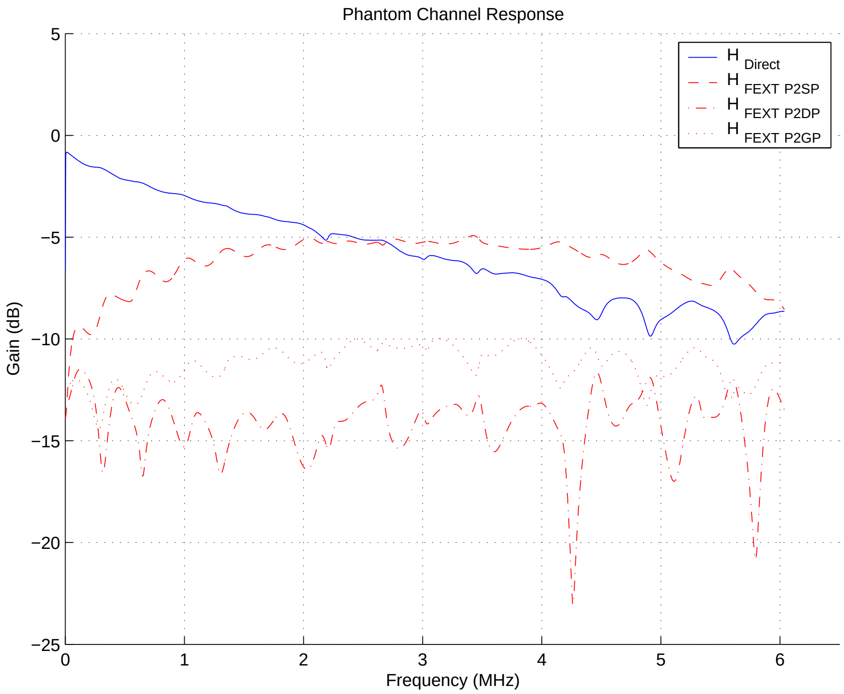

Figure 2.8: Magnitude response of a Phantom channel.

at a load resistance close to their characteristic impedance to minimize the signal power loss due to reflections.

2.3 Summery

In this chapter, measurement methodology for multiline measurement is provided. Introduction to basic transmission line parameters and a multiline model is discussed. The discussion is kept as simple as possible. Further we show the measured normal and Phantom channels to assist their comparison in later chapters.

Chapter 3

Channel Identification

The measurement data from the vector network analyzer are obtained in S-parameters and a transfer function was calculated from the data. The transfer function so obtained is a complex frequency response at a given frequency vector.

For a better understanding of the channel and that to be allowed to vary the frequency spacing (i.e. frequency grid), it is necessary to identify the channel in a closed form. We consider an identification process to find parametric models for the Phantom and normal channel response. For example, consider a rational polynomial transfer function in equation 3.1 to be a representation of the channel transfer function.

$$
\begin{aligned}
H(z) &= \frac{B(z)}{A(z)} \\
&= \frac{b_0 + b_1 z^{-1} + \ldots\ldots + b_N z^{-N}}{1 + a_1 z^{-1} + \ldots\ldots + a_N z^{-N}}
\end{aligned}
\tag{3.1}
$$

For $A = 1$, the rational polynomial transfer function takes the form of a finite impulse response transfer function. For $O(A) > 1$, the denominator polynomial is the characteristic polynomial of infinite impulse response transfer function.

3.1 Frequency Domain Vrs. Time Domain Identification

It is normally suggested to carry out the identification process on the raw data without any pre-processing on it. Since the measured data and the function response are in frequency domain, a time domain identification technique after conversion using frequency transform could be possible.

It was observed in many cases that time and frequency domain identification techniques give the equivalent model and can be obtained in either domain [28] and [29]. Irrespective of this duality, it is of interest to carry out the identification process in the same domain as of the data is measured. One such potential error can occur due to time domain leakage or wrap around error. Also the quantization error of data measurement with respect to their exact value and the added error due to conversion of data from one domain to the other can also be counted. There are few advantages parametric identification in frequency domain listed in [20] and the references therein.

One straightforward reason to use frequency domain identification is the nature of the channel. Copper channels are highly frequency selective. Errors in time domain identification process will be localized in time domain but will spread over all the frequencies in frequency domain. These errors will affect the frequency selective channel at all frequencies. On the other hand in frequency domain identification process the weighting at different frequencies can easily be implemented to more accurately identify the transfer function at the frequencies of interest.

3.2 Least Square Identification

We now formulate the problem of identifying a discrete filter by forming a least squares minimization problem. The idea is to find the coefficients of the rational transfer function of the form of equation (3.1).

The identification process assumes that the measurement errors are independently and identically distributed in the whole frequency range of measurement and that they are uncorrelated. Including the measurement noise term η in equatin (3.1),

$$H(z) = \frac{B(z)}{A(z)} + \eta. \tag{3.2}$$

In rational transfer function model to be estimated we assume that the noise term η is gaussian in nature. The model is identified using the methods of least squares. The coefficients $A(z)$ and $B(z)$ are chosen to minimize the equation error least square cost function,

$$\xi^{ls} = \frac{1}{2\pi}\int_0^{2\pi} W^{ls}(e^{j\omega})\left|\frac{B(e^{j\omega})}{A(e^{j\omega})} - H_m(e^{j\omega})\right|^2 d\omega \tag{3.3}$$

where,

$$H_N^m(e^{j\omega}) = \frac{Y_N(e^{j\omega})}{U_N(e^{j\omega})} \tag{3.4}$$

where $H_N^m(e^{j\omega})$ is the measured frequency response at N frequency points. This cost function is often referred as output error method. Let's consider the parameter vector Θ as,

$$\Theta = [b_0 \dots b_{N_B} \quad a_0 \dots a_{N_A}]^H \tag{3.5}$$

with

$$H^d(z, \Theta) = \frac{B(z, \Theta)}{A(z, \Theta)} \tag{3.6}$$

where, $H^d(z, \Theta)$ is the parameterized or desired frequency response model, and Θ_{N_p} *s.t.* $N_p = N_A + N_B + 1$, can be estimated with the least square estimator. The identification problem for the parameter vector Θ, is therefore,

$$\hat{\Theta} := \arg\min_{\Theta} \xi_N^{ls}(\Theta) \tag{3.7}$$

with

$$\xi_N^{ls}(\Theta) = \sum_{k=1}^{N} W^{ls}(e^{j\omega_k}) \left| \frac{B(e^{j\omega_k}, \Theta)}{A(e^{j\omega_k}, \Theta)} - H^m(e^{j\omega_k}) \right|^2 \tag{3.8}$$

This problem has been considered before [[23]] and several ways to solve this problem have been proposed [21],[22] and [26]. We shall consider briefly the cost function modifications made by Levy [21] and the frequency domain identification using Orthogonal Frequency Polynomials [26]. The later has attracted a lot of attention in the recent times.

3.2.1 Levy's Method

The least square identification problem stated in equation (3.7) is non-linear in nature. It can be calculated with a different weighting factor by modifying the non-linear nature of ξ^{ls} to a linear cost function, as suggested by Levy [21]. Since it is not exact least square cost function, it is also referred in various texts as equation error method. The two methods can be shown to be equivalent with a proper adjustment of the the weighting factors $W^{levy}(e^{j\omega})$ of ξ^{levy}.

The cost function ξ^{levy} for Levy's method is therefore modified as,

$$\xi^{levy} = \frac{1}{2\pi} \int_0^{2\pi} W^{levy}(e^{j\omega}) \left| B(e^{j\omega}) - A(e^{j\omega}) H^m(e^{j\omega}) \right|^2 d\omega \tag{3.9}$$

and accordingly, the identification problem of (3.7) can be restated as,

$$\hat{\Theta} := \arg\min_{\Theta} \xi_N^{levy}(\Theta) \tag{3.10}$$

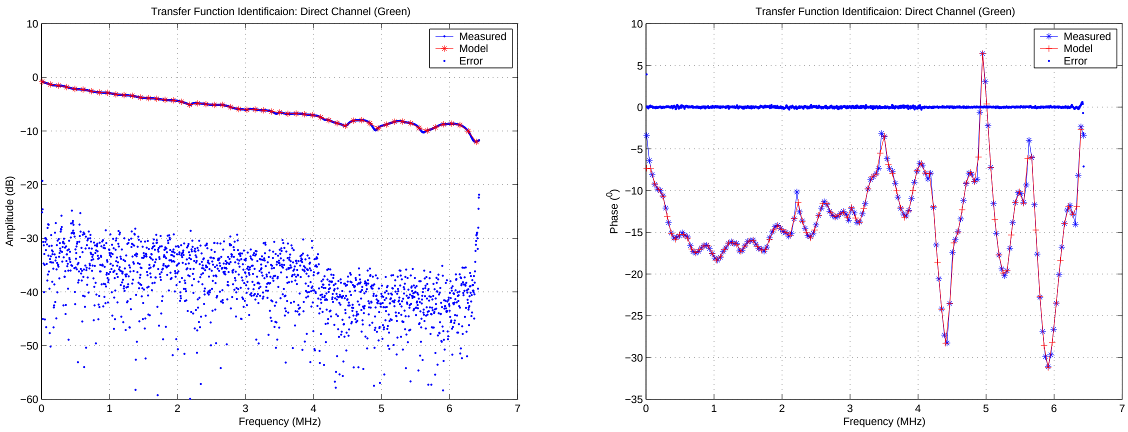

(a) Magnitude (b) Phase

Figure 3.1: (a)Magnitude and (b)Phase in Identification of a Phantom direct channel

with

$$\xi_N^{levi}(\Theta) = \sum_{k=1}^{N} W^{levy}(e^{j\omega_k}) \left| B(e^{j\omega_k}) - A(e^{j\omega_k}) H^m(e^{j\omega_k}) \right|^2$$

Another linear cost function was also proposed by Shanathanan [22]. We have used ξ^{levy} to estimate $A(e^{j\omega_k})$ and $B(e^{j\omega_k})$ and is discussed here. To solve this, we start by restating equation (3.10) in short-hand notation as,

$$\xi_{levy} = \sum_{k=1}^{N} w_k . |B(e^{j\omega_k}) - A(e^{j\omega_k}) . h_k^m|^2 \tag{3.11}$$

where ω_k is the $0 \leq \omega \leq 2\pi$, is the frequency grid at which measurements were performed. w_k is the short hand notation of $W(\omega_k)$, and $\Theta = \begin{bmatrix} \mathbf{b} \\ \mathbf{a} \end{bmatrix}$, with $\mathbf{b} = [b_0 \dots b_N]^H$ and $\mathbf{a} = [a_0 \dots a_N]^H$, where $(.)^H$ is used for Hermitian. Rearranging equation (3.11) as,

$$\xi_{levy} = \Theta^H \mathbf{\Psi} \Theta - \mathbf{\Phi}^H \Theta - \Theta^H \mathbf{\Phi} + \eta \tag{3.12}$$

where

$$\mathbf{\Psi} = \sum_{k=1}^{N} w_k \mathbf{e}_k \mathbf{e}_k^H, \quad \mathbf{\Phi} = \sum_{k=1}^{N} w_k h_k^m \mathbf{e}_k \quad \text{and} \quad \eta = \sum_{k=1}^{N} w_k |h_k^m|^2, \tag{3.13a}$$

$$\mathbf{e_k} = [1 \, e^{j\omega_k} \, e^{j*\omega_k} \dots e^{jN\omega_k} \quad -h_k^m e^{j\omega_k} \, - h_k^m e^{j2\omega_k} \dots - h_k^m e^{jN\omega_k}]^H. \tag{3.13b}$$

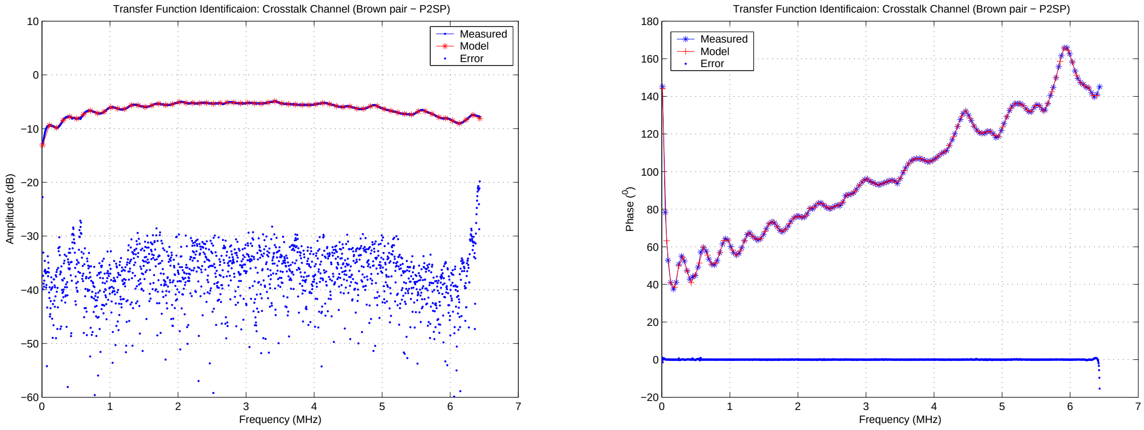

(a) Magnitude (b) Phase

Figure 3.2: (a)Magnitude and (b)Phase in Identification of a Phantom crosstalk channel

The cost function in (3.12) is quadratic in Θ and its solution is known to be [23],

$$\Theta = \Psi^{-1}\Phi \tag{3.14}$$

After solving equation (3.14) for Θ, the coefficient vectors a and b can be easily deduced. The channel response and the estimated response of direct channel are shown in Figure 3.1. The errors are plotted in dB for both magnitude and phase values. A crosstalk channel model is also shown in Figure 3.2.

3.2.2 Orthogonal Rational Polynomial Method

Along with Levy's method orthogonal rational polynomial method was also studied. These methods are becoming popular because a non-linear solution of equation (3.7) can be estimated more efficiently if the basis function is constrained to be orthogonal.

The orthogonal rational polynomial method converges faster and closer to $\hat{\Theta} \rightarrow \Theta$ with less parameters. It is obvious since for the transfer function (3.7) ORF is directly solved, while in Levy [21] or Sanathanan [22] method, a bias is introduced. The orthogonal rational polynomial (ORF) methods are computationally more complex than its biased counterparts. Since the computational power has tremendously increased, these methods are getting more attention.

A orthogonal basis was developed using Forsythe method [24] and implemented for the the identification in orthogonal space so generated. After the identification, the coefficients can be converted back from orthogonal basis space to the polynomial space of the independent variable. The method was first developed by Forsythe [24] and later discussed in [25].

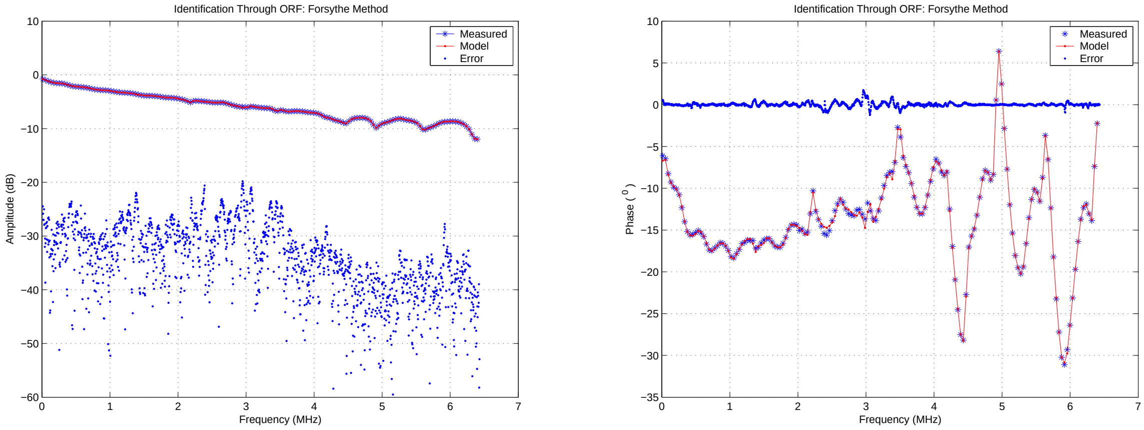

(a) Magnitude (b) Phase

Figure 3.3: (a)Magnitude and (b)Phase in Identification of a Phantom direct channel with Orthogonal Rational Transfer Function Method (See [24] and [25])

The results obtained by ORF - Forsythe fit method are shown for the same direct and crosstalk channel to provide a comparison. Figure 3.3. Recently generalized orthogonal rational fit have been proposed for the frequency domain identification [26].

In Figure 3.3 the noise is not as uniformly distributed as in the case of Levy's method in Figure 3.1. Since the identification were carried out offline, higher order were accepted for better identification in Levy's methods which was finally chosen for the identification in this chapter and ORF methods are not dealt in detail.

Goodness of Identification

In linear system identification the model order is defined as the highest power of z of the denominator of the transfer function in Equation (3.2). Increasing the model order directly affect the identification SNR between the measured and identified model. The noise term η, as assumed in Equation (3.2), is uniformly distributed over all frequencies and lower correlation between noise and signal indicates a better fit. It can be readily seen in Figure 3.4.

In Figure 3.4, under-modelling can be detected by the presence of non-gaussian noise η, low SNR and correlation between the measured and the noise signal, the difference of the estimated and measured transfer function. However it is emphasized that over-modelling would eventually increase the identification SNR but at the cost of tracking the noise present the signal. This would result in the modelling of measurement errors into the model as well. A moderate signal order should be accepted where the errors are uniformly distributed.

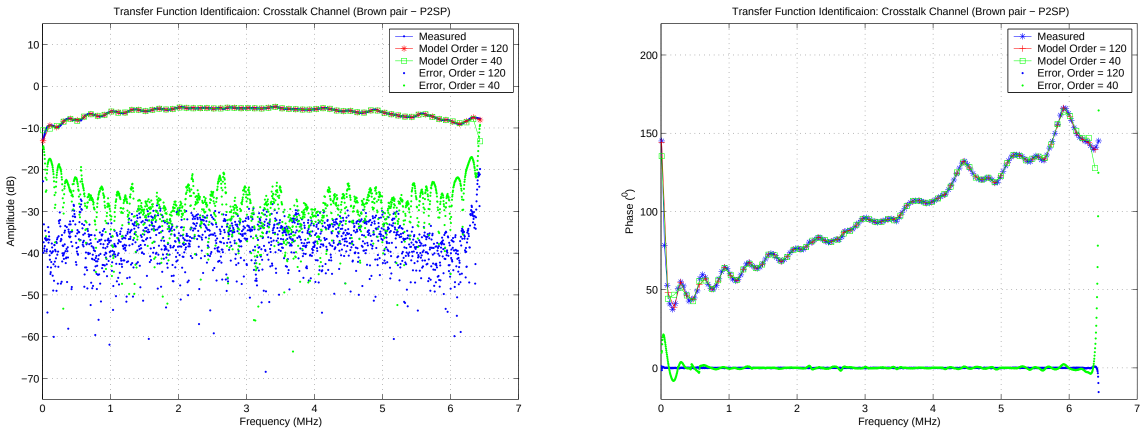

(a) Magnitude

(b) Phase

Figure 3.4: (a)Magnitude and (b)Phase in Identification of a Phantom direct channel for different order 120 (red) and order 40 (green)

3.3 Crosstalk Model Representation

Similar to ANSI [33] model for far-end crosstalk (FEXT), crosstalk models for Phantom FEXT are also studied. It is obvious that before concluding these FEXT models, large number of the experiments should be carried out. Various constants used in such empirical models should be statically supported by the set of these experiment. Nevertheless, to examine the kind of relationship they can exhibit, these representations were carried out.

As the crosstalk within different wire pair is different depending on the location of reference wire, in Phantom DSL FEXT crosstalk should be studied in the following four categories.

1. Crosstalk due to wire paired with ground wire *
2. Crosstalk due to wires in the same pair*
3. Crosstalk to another wire not in Phantom*
4. Crosstalk within two pairs not connected to the ground*

The first two can be understood for a simple phantom model of Figure 1.2. For the third type of crosstalk, we will assume an extension of Figure 1.2 to 5 Phantom wires with three pair used for the Phantom channel. In this case, the two pairs other than the pair which is twisted with the ground reference also exhibit crosstalk and which is different than the rest of the two type of crosstalk. For the ease of reference Figure 1.2 is reproduced here.

* As the number of experiments carried out were not sufficient, all these relations are approximate and not statistically verified. Moreover the relations, as can be seen from the corresponding figures, are not exact but are close to the crosstalks they refer to. More experiments are needed to predict such representations more efficiently.

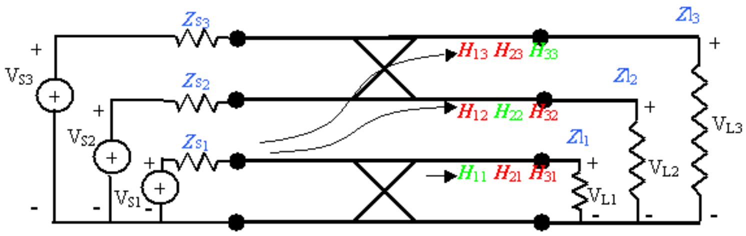

Figure 3.5: Phantom Mode (three active data-wires)

3.3.1 Crosstalk due to wire paired with ground wire

First consider the pair which shares a ground with one data wire and is equivalent to the normal mode if other Phantom pairs are removed. Consider H_{11} [see Figure 3.3] as the direct transfer function, than H_{12} and H_{13} will be very much similar except the difference how wire {2} and wire {3} of second pair interacts [Sec. 5.1.1]. An empirical model based on heuristics can be provided as,

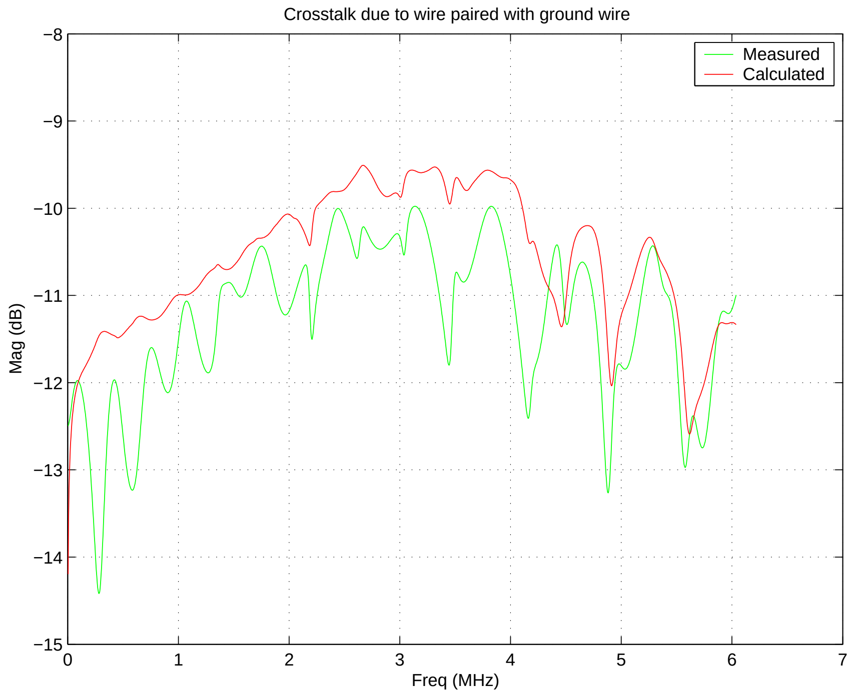

Figure 3.6: Crosstalk due to wire paired with ground wire

$$H_{12} = e^{-j\gamma(\phi,\tau,l,f)} \cdot k_{x1} \cdot H(f) \cdot f^{.18} \cdot d \cdot (1 + k_{x2} \cdot f \cdot sin(2\pi\ f/f_{s1})) \tag{3.15}$$

where,

$$k_{x1} = 21, \quad (3.16a)$$
$$k_{x2} = 6e-7, \quad (3.16b)$$
$$f_{s1} = 15\text{ MHz}, \quad (3.16c)$$
$$\gamma(\phi, \tau, l, f) = \text{A function of initial phase difference with respect to the crosstalker and twist densities of the two pairs under consideration, as explained in Figure 3.7.} \quad (3.16d)$$

Discussion on $\gamma(\phi, \tau, l, f)$

The obvious explanation of dependency of γ is followed from the transmission line theory. It is suggested in most of the ethernet installation that position of wire ends connecting to the RJ45 connectors should be controlled so that the initial phase difference ϕ can be minimized.

On the other hand, the twist densities of the crosstalker and the victim line will be another important component of this phase term. It is so because different twist length can give rise to different phase dependencies even if the initial phase ϕ is maintained exactly the same. It follows the obvious fact that the crosstalk within twisted pairs are a function of twists density.

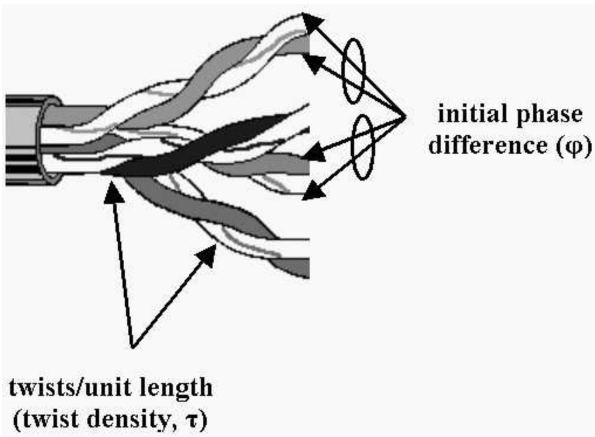

Figure 3.7: Initial Phase term ϕ and twist density τ

The dependencies of γ on ϕ and on τ, frequency(f), and, length of cable(l) can be given as,

$$\gamma(\phi, \tau, l, f) = c_1 \cdot \phi + f_n\left(\frac{\tau_{line1}}{\tau_{line2}}, l, f\right) \quad (3.17)$$

where the values of the constant c_1 and function 'f_n' are yet to be explored depending on their statistical behavior.

It is found that η is the FEXT that appears across the pair $\{2, 3\}$ when they are used in normal mode [See 5.1.2].

3.3.2 Crosstalk due to wires in the same pair

In a similar way, we can find the crosstalk within the same pair H_{23} and H_{32} as described in Figure 3.3. It is obvious that crosstalk within a pair would be maximum. A relationship can again be given by a similar relation as Eqn 3.15,

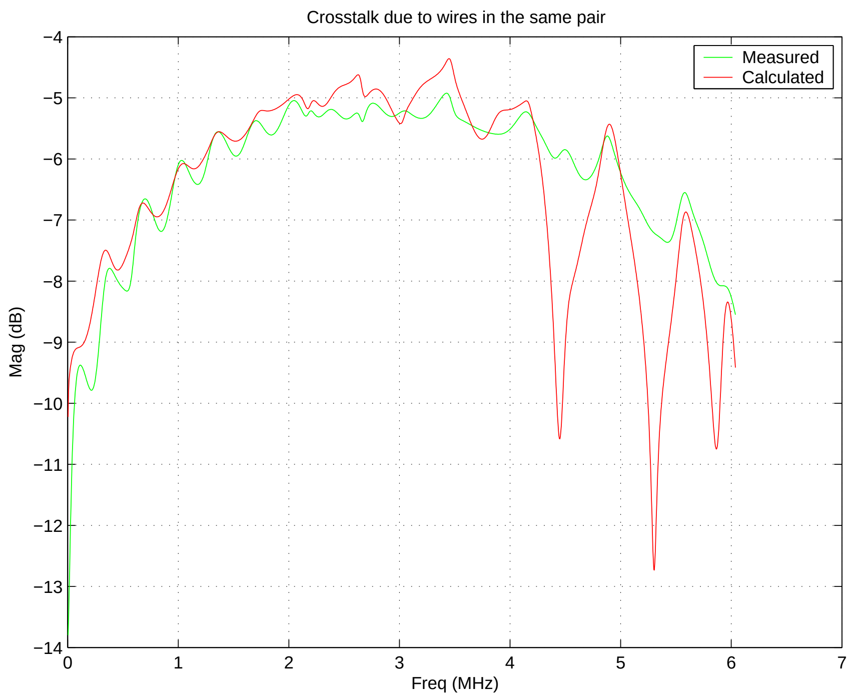

Figure 3.8: Crosstalk due to wires in the same pair

$$H_{23} = e^{-j\gamma(\phi,\tau,l,f)} \cdot k_{x3} \cdot H(f) \cdot f^{.18} \cdot d \cdot (1 + (k_{x4} \cdot f \cdot sin(2\pi\ f/f_{s1}))^{2/3}) \qquad (3.18)$$

where,

$$\begin{aligned} k_{x3} &= 45, \\ k_{x4} &= 1.8e-6, \\ f_{s1} &= 15 \text{ MHz}, \\ \gamma(\phi,\tau,l,f) &= \text{As in Eqn. 3.16, for wire pair \{2,3\}} \end{aligned}$$

A similar explanation of all the terms involved can be sought as in the previous section.

3.3.3 Crosstalk within two pairs not connected to the reference ground

This crosstalk appears only when $n \geq 3$ since in that case there are minimum two Phantom pairs none of which are twisted with ground. In this case all the four wires from two pairs are used for the data transmission and therefore all four wires under consideration gives rise to the crosstalk. This can be understood from Eqn. 5.1.2 or Eqn. **??**. This crosstalk can also be given in the similar fashion as in previous case,

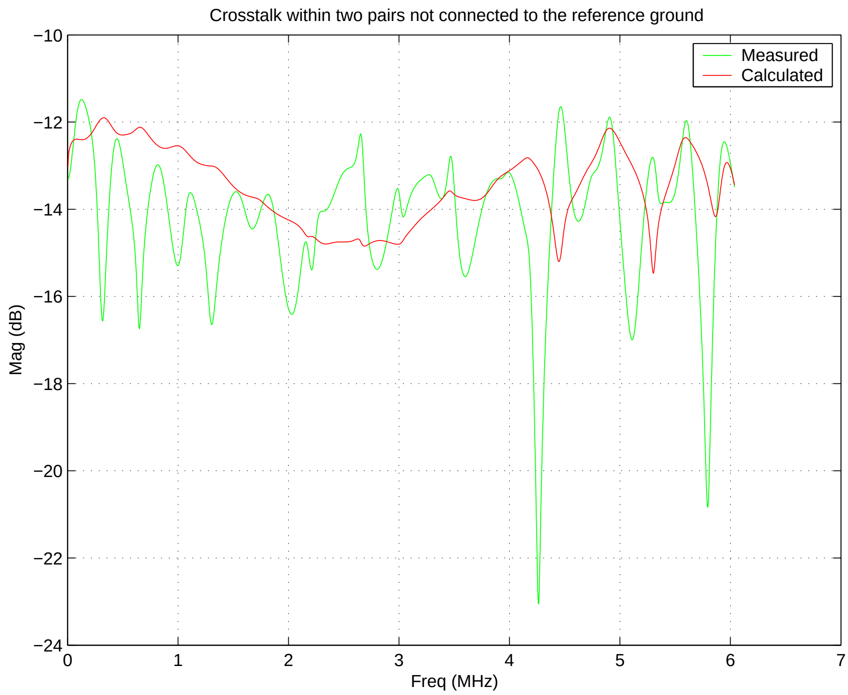

Figure 3.9: Crosstalk within two pairs not connected to the reference ground

$$H_{24} = e^{-j\gamma(\phi,\tau,l,f)} \cdot k_{x5} \cdot H(f) \cdot f^{.12} \cdot d \cdot (1 - k_{x6} \cdot f \cdot sin(4\pi\ f/f_{s1})) \quad (3.19)$$

where,

$$\begin{aligned} k_{x5} &= 1, \\ k_{x6} &= 2.8e-7, \\ f_{s1} &= 15 \text{ MHz}, \\ \gamma(\phi,\tau,l,f) &= \text{As in Eqn. 3.16, for wire pair } \{2,3\} \end{aligned}$$

Again in this case similar explanation of all the terms involved can be sought as in the previous section.

NOTE:

One might notice that the crosstalk response and their empirical expressions differ from figures. The aforementioned expressions assume an ideally terminated measurements and are based on heuristics. The measurements, as clear are not as smooth as their empirical expressions since they do not meet this condition. The port impedance mismatch in case of Phantom DSL is obvious as the port impedance could only be achieved either 50 *Ohms or* 100 *Ohms differential. While in Phantoms, as can be seen from Figure 2.6, the characteristic impedances are far more different than this ideal case. It is suggested that more measurements should be carried out before boiling down to these empirical expressions, though they should match closely. The newer set of measurements should be carried out using custom made Baluns (balanced to unbalance) to arbitrarily define a match between port and DUT impedances and minimize the reflections. Also note that for every combination of wire pairs, Baluns may have to be tailored according to the need. The accuracy of the measurement and prediction in terms of crosstalk will be greatly enhanced with the extensive use of Baluns.*

3.4 Summery

Channel identification cycle is discussed in least square sense in this chapter. Frequency domain identification is emphasized with the identification techniques by Levy and orthogonal rational transfer function estimation. Empirical expressions for various crosstalk in Phantom DSL is also provided. However, it is to be noted that these empirical expressions are subjected to modification after statistical studies of the behavior of these crosstalks.

Chapter 4

Capacity Comparison : Phantom vs. Normal DSL

As explained in section 1.3 the main purpose of these measurements and identification process is to draw a comparison and present the capacity gains of Phantom mode DSL over normal DSL. To this end, this chapter provides a simple formulation for the Phantom mode DSL capacity and compare it with normal mode DSL capacity in no-crosstalk cancelation and full crosstalk cancelation scenarios. In the end the possibilities of gigabit transmission on subscriber loops is also discussed.

4.1 Capacity Formulation in Normal and Phantom DSL

We start with the assumption of a gaussian channel H, i.e. the noise samples are uncorrelated and gaussian distributed over all frequencies. Consider a channel with channel response,

$$\mathbf{y} = H\,\mathbf{x} + \mathbf{n}, \tag{4.1}$$

where $\mathbf{y}$ is the output vector, $\mathbf{x}$ is the input vector and $\mathbf{n}$ is the vector Gaussian noise. H is the channel matrix. It is assumed that the noise vector is independently and identically distributed (iid). The info-theoretic capacity of such a channel in a frequency band $[f_1, f_2]$ is given by Shannon's channel capacity theorem as,

$$C = \int_{BW} \log_2\left(1 + \frac{S(f)}{N(f)}\right) df \qquad \text{bit/s}, \tag{4.2}$$

where $S(f)$ is signal power density while $N(f)$ is the noise power density. In DSL the noise power density includes the noise from crosstalk sources and can be given as,

$$N(f) = N_{NEXT} + N_{FEXT} + N_{AWGN}$$

We do not consider impulse and RFI noise in the following discussion. They can be dealt independently from the crosstalk. A more realistic estimate of capacity is in terms of capacity per bandwidth unit η and is measured in bits/s/Hz. Rearranging 4.2 as,

$$\eta = \frac{C}{W} = \log_2\left(1 + \frac{S(f)}{N_{NEXT} + N_{FEXT} + N_{AWGN}}\right) \qquad \text{bit/s/Hz}, \tag{4.3}$$

The NEXT can be avoided employing frequency division duplexing (FDD) for DMT modulated systems as DSL. Also additive white gaussian noise (AWGN) in DSL is assumed to be −140dBm/Hz [1]. FEXT remains the main contribution of frequency dependent noise. In case of Normal DSL, the spectral efficiency in 4.3 is disturbed by the normal mode crosstalk. In Phantom, however, the crosstalk has other constituents within the Phantom DSL itself as mentioned in 3.3. In the new scenario,

$$N_{FEXT} = N_{\text{same pair}} + N_{\text{different pair}} + N_{\text{ground pair}} + N_{\text{alien}} \tag{4.4}$$

or equivalently for n pair phantom,

$$N_{FEXT} = |H_{\text{same pair}}|^2 + \sum_{i=1}^{2n-3} |H_{\text{different pair}}|^2 + |H_{\text{ground pair}}|^2 + \sum_{\substack{\text{over all alien}\\ \text{crosstalkers}}} |H_{\text{alien}}|^2 \tag{4.5}$$

where $N_{\text{same pair}}$ is the crosstalk arising due to the signals in adjacent wire within the same pair and is equivalent to H_{23} in sec. 3.3. Similarly $N_{\text{different pair}}$ and $N_{\text{ground pair}}$ are the crosstalks arising from the signals in the other wire in Phantom not paired with the ground reference and paired with the ground reference wire respectively. They are denoted as H_{24} and H_{12} in sec. N_{alien} is the alien crosstalk. 3.3 respectively. The relation 4.3 is modified accordingly in Phantom DSL.

$$\eta_{\text{Phantom}} = \log_2\left(1 + \frac{S(f)}{N_{\text{same pair}} + N_{\text{different pair}} + N_{\text{ground pair}} + N_{\text{alien}} + N_{AWGN}}\right) \qquad \text{bit/s/Hz}, \tag{4.6}$$

Also note that, if the number of pairs used in Phantom DSL are n, the only term that is modified in 4.6 is $N_{\text{different pair}}$ which will be should be multiplied by $n-2$ to account for the power sum crosstalk due to all other crosstalking pairs within Phantom. In the following, the background noise is assumed to be white and with a power spectral density (PSD) of -140dBm/Hz. Also the capacity for each channel in Phantom can be calculated and summed to give the total capacity of the Phantom, which can be alternatively given as a MIMO capacity as in Sec. 4.1.1. The reference PSD of the transmitter power for the purpose of SNR calculations is set to a flat PSD of −60 dBm/Hz. For the purpose of clarity, only average channel SNR and capacities are shown in this text.

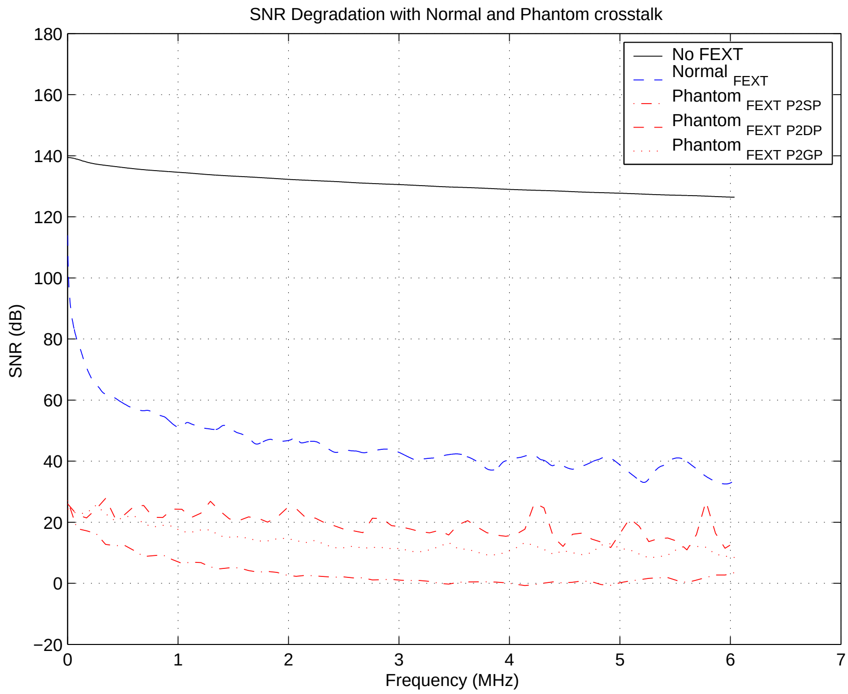

Figure 4.1: Comparing the Signal-to-Noise Ration of a normal and Phantom Channel

4.1.1 Phantom and Normal DSL as MIMO Channels

As mentioned in Sec. 1.3 and in 2.1.1, Phantom DSL can be realized using MIMO transmission techniques. Much in a similar way, bonded DSL loops can also be realized as MIMO. In this case the capacity of a MIMO DSL of dimension n can be given by,

$$C_{\text{MIMO}} = \int_{BW} \log_2 \left[det \left(\mathbf{I} + \frac{\rho}{n} \mathbf{HH}^* \right) \right], \tag{4.7}$$

or alternatively it can also be shown that the average capacity of MIMO increases linearly with the number of lines n;

$$\eta_{\text{MIMO}} \approx n \ \log_2 (1 + \rho), \tag{4.8}$$

The capacity gains are obvious in Phantom DSL with the increase in the number of channels from n normal DSL with same number of pairs involved in MIMO channel realization to $2n - 1$ in Phantom DSL.

4.2 Signal to noise ratio comparison

The first step is to recognize the signal-to-noise-ratio (SNR) in Phantom Mode and Normal mode. It is assumed that the crosstalk noise is the only source of the noise present in the DSL system considering that impulse noise and RFI are independent to the crosstalk. It is obvious that in phantom mode, the various crosstalker among different lines sum up and the total crosstalk is much more than the normal mode DSL [Equation 4.6]. It is intuitive that we assume the power-sum effect of these corsstalks on the direct channel response in SNR calculations. The Signal to noise ratio of Normal and Phantom DSL are compared and represented in Figure 4.1. The figure shows that the SNR remains relatively unaffected in Normal DSL once affected by crosstalk. On the other hand a drastically low SNR is obtained on lines which are not paired with the ground. The SNR gains of Normal DSL are obvious over Phantom DSL. Capacities of Normal and Phantom DSL are compared in the next section.

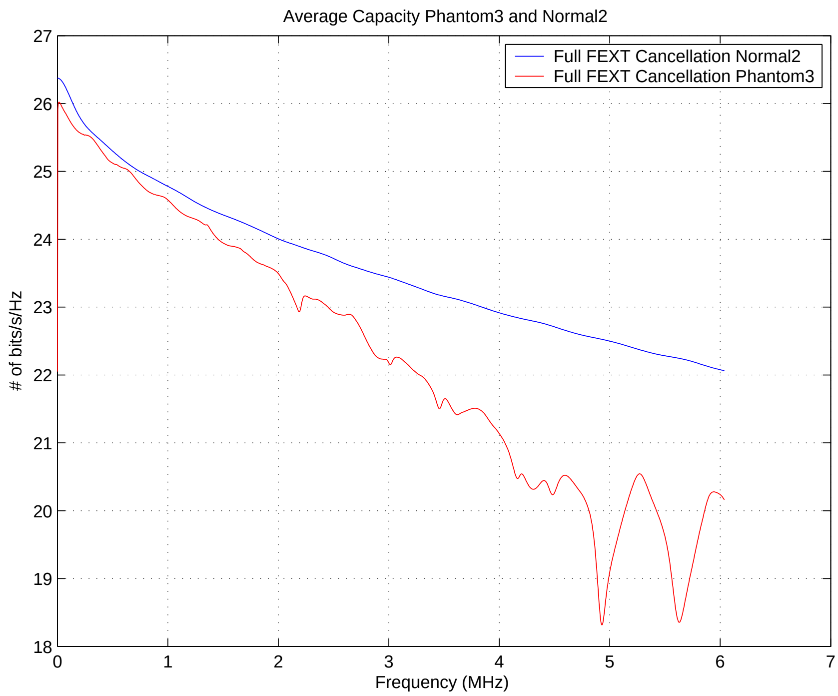

Figure 4.2: Capacity comparison between 2 Normal Channels and a Phantom Channel of dimension 3 (2-pairs)

4.3 Capacity Comparison

In capacity comparison we assume full crosstalk cancelation and that the channel is gaussian with white (thermal) noise of a PSD equal to -140 dBm/Hz. It predicts the gains in terms of channel capacity in Phantom DSL against the Normal DSL. It must be kept in mind that the Figure 4.2 and 4.3 gives the average capacity per available channel with same number of twisted pair involved. The Phantom, if full crosstalk cancellation is achieved, can provide almost double the data rates as $2n - 1$ data channels are available against only n in normal DSL. In coordinated DSL system the crosstalk can be completely mitigated in Phantom DSL

[32] and a huge gain in the phantom channel capacity is obvious. Towards the end of this chapter, gigabits on DSL loops is briefly discussed.

It is assumed that a flat PSD of −60 dBm/Hz is applied at the transmitter. Table 4.1 summarizes the parameters used [35] for the capacity calculations and the cable specifications.

Loop Length	305m
Cable Type	24 AWG(0.5mm) (4 pairs, Cat5e)
Tone width	4312.5 Hz
Symbol Rate	4000 Hz
Symbol error probability	10^{-7} or less
Coding gain	3.5 dB
Noise Margin	6.0 dB
Transmit PSD	-60 dBm/Hz

Table 4.1: Cable and Simulation parameters

As plotted in Figure 4.2, it shows the capacities of Phantom DSL with 2 twisted pairs pairs i.e. 3 data channels for Phantom3. Figure 4.3 shows the capacity gains in Phantom5.

From the discussion it is clear that for such crosstalk mitigation, coordination among the Phantom line is necessary. Therefore, a coordinated MIMO channel methods (see [10], [32]) can be employed to exploit the huge capacity gains of Phantom DSL. A new method of Per-tone crosstalk cancellation is also discussed in [30], which allows full cancellation of the crosstalk from a multi-user channel with only one ended joint signal processing.

4.4 Gigabit on Copper Lines

As fiber is reaching closer to the customer premise, the interests of higher data rate at shorter lengths is also increasing with application of joint signal procession at CO/ONU. Gigabit DSL was originally proposed as an extension of [5] and [2] and is sought to deliver a minimum of 1 Gbps at shorter lengths by John Cioffi (see [31]). It is motivated from 1G and 10G Ethernet protocol and is supposed to provide an alternative at longer run lengths.

In Ethernet technology, a cable of 4 pair, Cat 5e or lower is used for run lengths of ∼ 100 to ∼ 150 meters. While using similar cables in Phantom as in Figure 4.4, 7 parallel Phantom channels are available. For such short lengths, it can be assumed that the cables are provided from a central point to different places in a residential or commercial place. The channels can be treated independently if they do not run together in a bundle and the power sum crosstalk

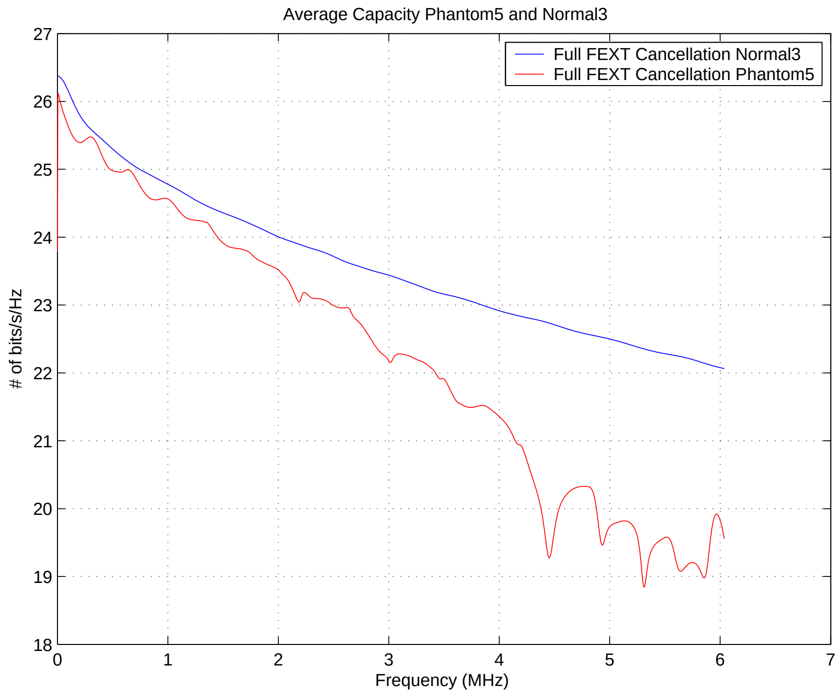

Figure 4.3: Capacity comparison between 3 Normal Channels and a Phantom Channel of dimension 5 (3-pairs)

[see 5.2] would not be very strong. Also assume that a fully coordinated MIMO scheme is applied to these Phantom channels, a capacity is drawn in table 4.2. It is obvious that in such a scenario gigabit DSL can be realized with MIMO schemes.

Numbers of DMT Tones	Capacity (Mbps), 4-pairs Phantom7 | Normal4		Capacity (Mbps), 2-pairs Phantom3 | Normal2	
256	151.1	86.4	64.8	43.2
512	294.9	168.5	126.4	84.3
1024	567.9	324.5	243.4	162.3
2048	1072.3	612.6	459.6	306.4
4096	1960.4	1120.3	840.2	560.1

Table 4.2: Comparison of the Phantom and normal DSL MIMO capacities

A comparison of the maximum possible data rates in fully coordinated environment is presented here. It is obvious from the achievable data rate that with same number of twisted pairs, Phantom can deliver much higher data rate at the same length. Another advantage in Phantom would be due to full MIMO applications since it is inherent in the assumption that all the Phantom lines originate from the same place and reaches to a same place, giving

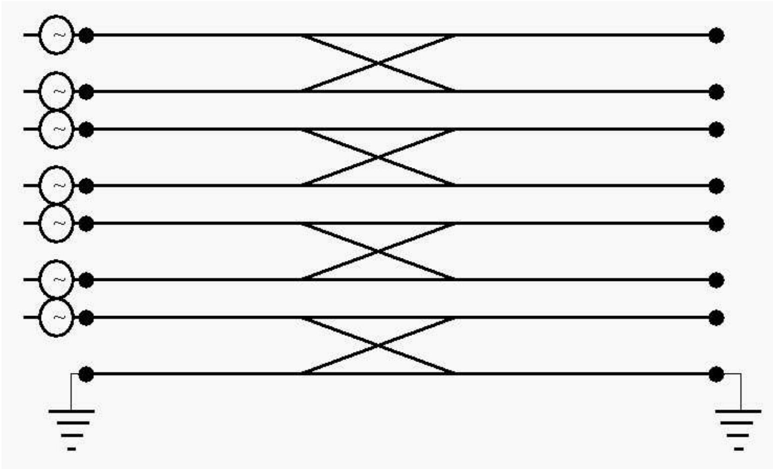

Figure 4.4: A rough prototype of GDSL topology of 4 pairs sharing one arbitrarily choosen ground and the rest of the wires are used in Phantom.

opportunity to fully exploit the channel information at both receiver and transmitter side. In normal DSL, however these high data rates are difficult to obtain due to the huge crosstalk and no perfect crosstalk cancelation algorithm in distributed multi-user environment is known yet.

From the capacity comparison in Table (4.2), it is clear that Phantom7 (4-pair cable) with 2048 tones sum up to give a Gigabit data rate in the ideal case. Similarly for Phantom3 (2-pairs), a Phantom line can deliver as much as $\tilde{8}40$ Mbps at 300 meters with 4096 tones. Since the attenuation at lower distances is less, even more number of tones can be used for the transmission and considerable gains in data rate can still be achieved.

4.5 Summery

The motivation behind these studies was to provide a comparison between Normal DSL to Phantom DSL techniques. It is readily seen that the crosstalk in Phantom is severely high when compared to Normal DSL. However, it should be noted that the capacity gains on the same number of wires for 2 or more normal DSL pairs, have high advantage in Phantom DSL if the crosstalk is eliminated. This comparison highlights the need to investigate methods to reduce the crosstalk in Phantom DSL. MIMO communication techniques give more insight to such methods and needed to be studied in details. [10] and [30] base their crosstalk cancelation on per-tone vectored transmission techniques.

Chapter 5

On the relation of Phantom and Normal Channels

It is of great interest to see the relationship between Phantom channels and Normal DSL channels. Exploring the relationship, we describe a natural phenomena of electromagnetic coupling between a Phantom channel matrix to a Normal channel matrix.

In twisted pairs, the electromagnetic fields generated due to the currents in opposite direction, and therefore, magnetic dipoles in opposite direction result in the cancelation of crosstalk or and the reduction of the strength of interference of the signal from one line to another. At moderate frequencies, where the length of copper conductor is comparable to the wavelength or smaller, lumped model is found to be very close to the natural physical process of electromagnetic coupling that occurs in transmission lines. At higher frequencies, however, longer copper cables are no more well represented by lumped model as the wavelength of the becomes smaller than the line length, giving rise to higher crosstalk at higher frequencies. The normal line parameters R, L C and G do not follow the lumped model and it is not easy to compensate externally in the present settings accurately. As the frequency of transmission increases, the effective length of the copper cable which can carry data, reduces.

The other reason for the crosstalk in twisted pair is the non-perfect symmetry of the twists per unit length and their density. More densely and uniformly twisted pair cables have less crosstalk and is the central point in the development of low crosstalk twisted copper pair categories. This is also the key point of understanding the crosstalk behavior and their relations between Phantom and Normal channel, as explained in section 5.1.

In this chapter we will discuss the relationship of phantom channel matrix to that of normal channel matrix and the power sum crosstalk of phantom DSL in a cable where other DSL variant technologies are deployed. It is possible to reduce the effect of the crosstalk at the cost of higher computational complexity. A method is proposed in [30] and is highly robust in distributed multi-user DSL environment.

5.1 Phantom vs. Normal Channel Matrices

As stated earlier, it is of interest to see how phantom mode channel matrix transfer function relate to the normal mode channel matrix. Let H_{ij}^{P} be the transfer function of wire (i, j) in phantom mode while H_{ij}^{N} be the transfer function in normal mode for (i,j)th pair. We want to explore a relation $\mathbb{O}$ between the two channel matrices such that,

$$\begin{bmatrix} \mathbf{H}_{1,1}^{P} & \mathbf{H}_{1,2}^{P} & & \cdots & \mathbf{H}_{1,2n-1}^{P} \\ \mathbf{H}_{2,1}^{P} & \ddots & & & \vdots \\ \vdots & & \ddots & & \vdots \\ \vdots & & & \ddots & \vdots \\ \vdots & & & & \vdots \\ \mathbf{H}_{2n-1,1}^{P} & & \cdots & & \mathbf{H}_{2n-1,2n-1}^{P} \end{bmatrix} \overset{\mathbb{O}}{\Longrightarrow} \begin{bmatrix} \mathbf{H}_{1,1}^{N} & \mathbf{H}_{1,2}^{N} & \cdots & \mathbf{H}_{1,n}^{N} \\ \mathbf{H}_{2,1}^{N} & \ddots & & \vdots \\ \vdots & & \ddots & \vdots \\ \mathbf{H}_{n,1}^{N} & \cdots & & \mathbf{H}_{n,n}^{N} \end{bmatrix} \tag{5.1}$$

We will use simple notation for $2n-1 \times 2n-1$ phantom channel matrix $[\mathbf{a}_1, \mathbf{a}_2 \ldots \mathbf{a}_{2n-1}]$, where $\mathbf{a}_1 = [a_{1,1}, a_{2,1} \ldots a_{2n-1,1}]^T$. A possible transformation from this matrix to an $n \times n$ normal channel matrix would be to reduce the columns and rows of the wires which will be used as ground/reference wires in the normal mode channel.

5.1.1 Phantom3 and Normal2:

We start with the simplest case of $n = 2$ and a transformation $\mathbb{O}$ such that it reduce the 3×3 phantom channel matrix to the 2×2 normal mode channel matrix. Let's start with considering a 3×3 phantom channel,

$$\mathbf{A} = \begin{bmatrix} a_{1,1} & a_{1,2} & a_{1,3} \\ a_{2,1} & a_{2,2} & a_{2,3} \\ a_{3,1} & a_{3,2} & a_{3,3} \end{bmatrix} \tag{5.2}$$

where $a_{1,1}$ is the direct response of the wire 1 which shares a ground within the same pair. $a_{2:3,2:3}$ belongs to a single pair and the response is measured with respect to the reference which is paired with wire 1. If we assume the following operation,

$$\mathbf{TAT}^T = \begin{bmatrix} a_{1,1} & a_{1,2} - a_{1,3} \\ a_{2,1} - a_{3,1} & a_{2,2} - a_{2,3} - a_{3,2} + a_{3,3} \end{bmatrix} \tag{5.3}$$

where $\mathbf{T}$ is a transformation matrix given as,

$$\mathbf{T} = \begin{bmatrix} 1 & 0 & 0 \\ 0 & 1 & -1 \end{bmatrix} \tag{5.4}$$

Discussion on Transformation Matrix: The choice of transformation matrix is very straightforward. Fig. 1.2 shows that the line 2 and 3 belongs to the same pair. In normal mode one of the two will be referred as the ground/reference wire. While from transmitter, this is made zero, on the receiver we measure the response in differential mode between lines 2 and 3, and therefore, the transforation matrix reflect that differential measurement between these two lines. Thus the transformation matrix **T** is the simplified forme of the following,

$$\mathbf{T} = \begin{bmatrix} 1 & 0 & 0 \\ 0 & 1 & -1 \end{bmatrix} \equiv \begin{bmatrix} 1 & 0 & 0 \\ 0 & 1 & -1 \\ 0 & 0 & 0 \end{bmatrix} \tag{5.5}$$

Discussion on Transformed Matrix: The transformation $\mathbf{TAT}^T$ is equivalent to the normal channel **B** (for simplicity) with the following modifications,

$$a_{2,3} = a_{3,2} = a_{3,3} = 0 \tag{5.6}$$

To emphasis on that these elements are indeed zero, we will adopt a block wise approach. Referring back to the Figure [1.2], line 2 and 3 belong to the same pair, while in normal mode one of the lines will be set to the reference voltage at the transmitter as explained in the previous discussion. It is obvious that any crosstalk between these two line ($a_{2,3}$ and $a_{3,2}$ in this case) will vanish. On the other hand, the term related to the direct response of the line which is used as reference will also vanish, say line 3 in this case reducing the term $a_{3,3}$ to zero. It follows that,

$$\mathbf{B} = \begin{bmatrix} b_{1,1} & b_{1,2} \\ b_{2,1} & b_{2,2} \end{bmatrix} = \begin{bmatrix} a_{1,1} & a_{1,2} - a_{1,3} \\ a_{2,1} - a_{3,1} & a_{2,2} \end{bmatrix} \tag{5.7}$$

For the cross terms, it is not so obvious and an explanation is sought here. Going through the cross terms, it appears as the crosstalk between the two pairs is due to the difference of $a_{1,2} - a_{1,3}$ and on the other side due to $a_{2,1} - a_{3,1}$. The electromagnetic coupling of the first pair with each wire of the second pair is different. The difference of the two responses gives rise to the crosstalk between the two pairs. If the electromagnetic coupling of the first pair with each wire of the second pair had been the same, there had been no crosstalk as it had been canceled due to equal opposite direction of electric current and therefore of the magnetic dipole arising due to flow of charge(current). Since it is not so, this difference of the electromagnetic coupling gives rise to the crosstalk between the two pairs. It will be more obvious when we study the higher dimension of the Phantom mode, where the normal mode crosstalk between different pairs comes as a natural extension of this phenomena.

5.1.2 Phantom5 and Normal3:

Let us consider a case of $n = 3$, i.e. in normal mode 3 DSL lines are available while in Phantom mode $2 \times 3 - 1 = 5$ lines are available. Continuing with the same notation as used in the previous discussion, consider a similar Phantom channel **A**, Normal channel **B** and transformation **T**,

$$\mathbf{A} = \begin{bmatrix} a_{1,1} & a_{1,2} & a_{1,3} & a_{1,4} & a_{1,5} \\ a_{2,1} & a_{2,2} & a_{2,3} & a_{2,4} & a_{2,5} \\ a_{3,1} & a_{3,2} & a_{3,3} & a_{3,4} & a_{3,5} \\ a_{4,1} & a_{4,2} & a_{4,3} & a_{4,4} & a_{4,5} \\ a_{5,1} & a_{5,2} & a_{5,3} & a_{5,4} & a_{5,5} \end{bmatrix} \tag{5.8}$$

$$\mathbf{B} = \begin{bmatrix} b_{1,1} & b_{1,2} & b_{1,3} \\ b_{2,1} & b_{2,2} & b_{2,3} \\ b_{3,1} & b_{3,2} & b_{3,3} \end{bmatrix} \tag{5.9}$$

$$\mathbf{T} = \begin{bmatrix} 1 & 0 & 0 & 0 & 0 \\ 0 & 1 & -1 & 0 & 0 \\ 0 & 0 & 0 & 1 & -1 \end{bmatrix} \tag{5.10}$$

After applying the transformation $\mathbf{TAT^T}$ to the phantom channel,

$$\mathbf{B} = \mathbf{TAT^T} = \begin{bmatrix} a_{1,1} & a_{1,2} - a_{1,3} & a_{1,4} - a_{1,5} \\ a_{2,1} - a_{3,1} & a_{2,2} - a_{2,3} - a_{3,2} + a_{3,3} & a_{2,4} - a_{3,4} - a_{2,5} + a_{3,5} \\ a_{4,1} - a_{5,1} & a_{4,2} - a_{5,2} - a_{4,3} + a_{5,3} & a_{4,4} - a_{5,4} - a_{4,5} + a_{5,5} \end{bmatrix} \tag{5.11}$$

Further, without any loss of generality,

$$a_{2,3} = a_{3,2} = a_{3,3} = 0, \tag{5.12a}$$

$$a_{4,5} = a_{5,4} = a_{5,5} = 0 \tag{5.12b}$$

which reduces 5.11 to,

$$\mathbf{B} = \begin{bmatrix} a_{1,1} & a_{1,2} - a_{1,3} & a_{1,4} - a_{1,5} \\ a_{2,1} - a_{3,1} & a_{2,2} & a_{2,4} - a_{3,4} - a_{2,5} + a_{3,5} \\ a_{4,1} - a_{5,1} & a_{4,2} - a_{5,2} - a_{4,3} + a_{5,3} & a_{4,4} \end{bmatrix} \tag{5.13}$$

$b_{1,i}$ and $b_{i,1}$, $\forall\, i = 1, 2, 3$ can be explained in the same way as in the previous case. The crosstalk terms between pairs consisting Phantom lines {2,3} and {4,5} are more involved but can be explained in the same way as for pairs consisting Phantom lines {1} and {2,3} in the previous case.

Let's focus on the term $b_{2,3}$. Writing $b_{2,3}$ again and rearranging as,

$$\begin{aligned} b_{2,3} &= a_{2,4} - a_{3,4} - a_{2,5} + a_{3,5} \\ &= (a_{2,4} - a_{3,4}) - (a_{2,5} - a_{3,5}) \\ &= \text{Electromagnetic coupling of pair } \{2,3\} \text{ with } \{4\} \\ &\quad - \text{Electromagnetic coupling of pair } \{2,3\} \text{ with } \{5\}. \end{aligned} \tag{5.14}$$

As discussed in the previous section that the electromagnetic coupling of pair $\{2,3\}$ with $\{4\}$ and $\{2,3\}$ with $\{5\}$ essentially give the same information. Opposite sign should indicate that One of the two terms can therefore be dropped without any loss of information as,

$$a_{2,5} = a_{3,5} \quad = 0. \tag{5.15}$$

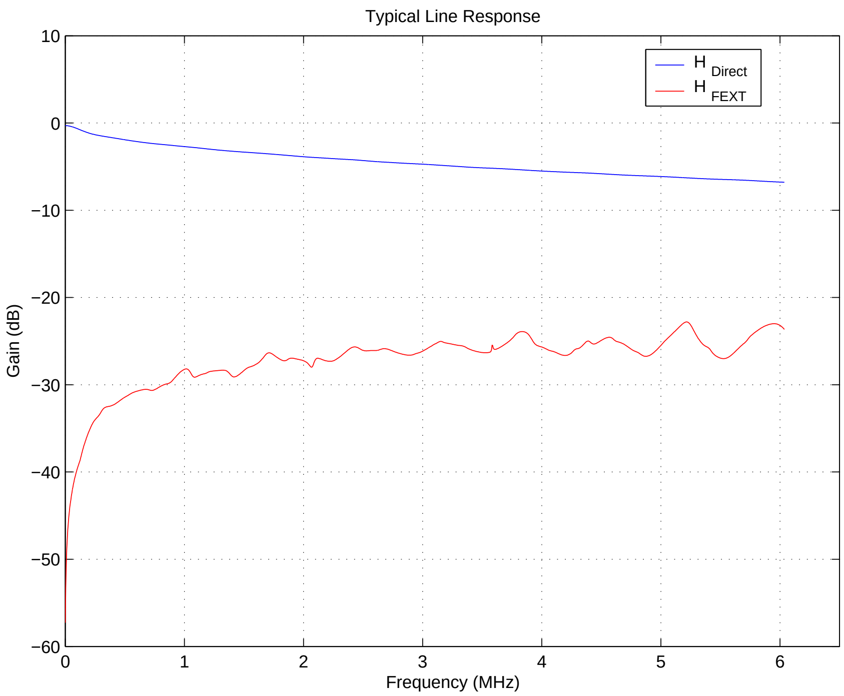

Figure 5.1: Normal DSL Channel

A similar explanation can be given for $b_{3,2}$, which again reduces to the similar term. Thus, the obtained matrix should give information about the normal DSL channel, if applied to the

Phantom pairs to form a normal channel.

Following the discussion above, we find that the essential transformation in the following form,

```
Algorithm 1 : Phantom to Normal
--------------------------------

    // Make Block Diagonal as explained in Equation 5.12

    For  i >= 2:2:2n-1;
        Select Paired Phantom Blocks as B(i:i+1,i:i+1),
        Set B(i,i+1) = B(i+1,i) = B(i+1,i+1) = 0;
    End

    // For Example
    // /                     \     /               \
    // | a(i,i)    a(i,i+1)   |     | a(i,i)    0   |
    // |                      |  =  |               |
    // | a(i+1,i)  a(i+1,i+1) |     |   0       0   |
    // \                     /     \               /
    //

    // Make Off-diagonal as explained in Equation 5.15

    For  i >= 2:2:2n-1;
        For j = (2:2:2n-1) and (j NOT-EQUAL i)
            Select Blocks as B(i:i+1,j:j+1),
            Set B(i,j+1) = B(i+1,j+1) = 0;
        End
    End

    // For Example
    // /                     \     /                   \
    // | a(i,j)    a(i,j+1)   |     | a(i,j)       0    |
    // |                      |  =  |                   |
    // | a(i+1,j)  a(i+1,j+1) |     | a(i+1,j)     0    |
    // \                     /     \                   /
    //

    // Choose the Transformation Matrix T such that,
```

```
//         |
//         | T(1,1) = 1;
// T   =   | T(i=2:1:n-1,j=2*i-2) = 1  ;
//         | T(i=2:1:n-1,j=2*i-1) = -1 ;
//         | Otherwise 0

// And Apply the following transformation

B = T * A * Transpose(T);   \\ Normal DSL Channel
```

Looking at the individual crosstalk terms of **B**, and comparing them with the Normal channel matrix 5.1.3. It is obvious that there exist a definite relation between the crosstalk between the pairs in normal mode and in phantom mode of DSLs. It should always be possible to find the normal DSL channel if the information of phantom channel is available.

5.1.3 Simulation

The phantom channel and normal channel are separately measured and plotted in Figure 5.2 and in Figure 2.7. The relation discussed here has been deduced and compared against the measured channel response of normal channel in Figure 5.3 .

5.2 Disturbance to a Nearby Victim Line

It is obvious that the high crosstalk is inherent to the Phantom DSL. The crosstalk within Phantom pairs can be mitigated using MIMO techniques and multi-user detection as described in [30] and [11]. But it is interesting to learn about the disturbance to services in the same cable by a Phantom DSL. More so, since Phantom DSL is supposed to work at the same frequencies as its predecessors like ADSL and VDSL. The crosstalk from stand alone single A/VDSL loops (normal DSL) can be defined as the power sum FEXT as seen by the victim line in the vicinity.

As demonstrated in the previous section 5.1.2, in equation 5.13, the crosstalk to another pair can also be similarly explained in case of Phantom channel. The green, brown and blue pairs were used in the Phantom mode and the orange pair was used to measure the crosstalk in all cases for measurement. It is noticed that the victim line experiences a linear increase in the crosstalk from Phantom as the number of parallel line increases in a Phantom DSL.

The crosstalk from a phantom DSL to the nearby DSL loops can be seen as a power sum crosstalk in this case also. Lets consider a simple case of Phantom of 2 wire pairs, consisting

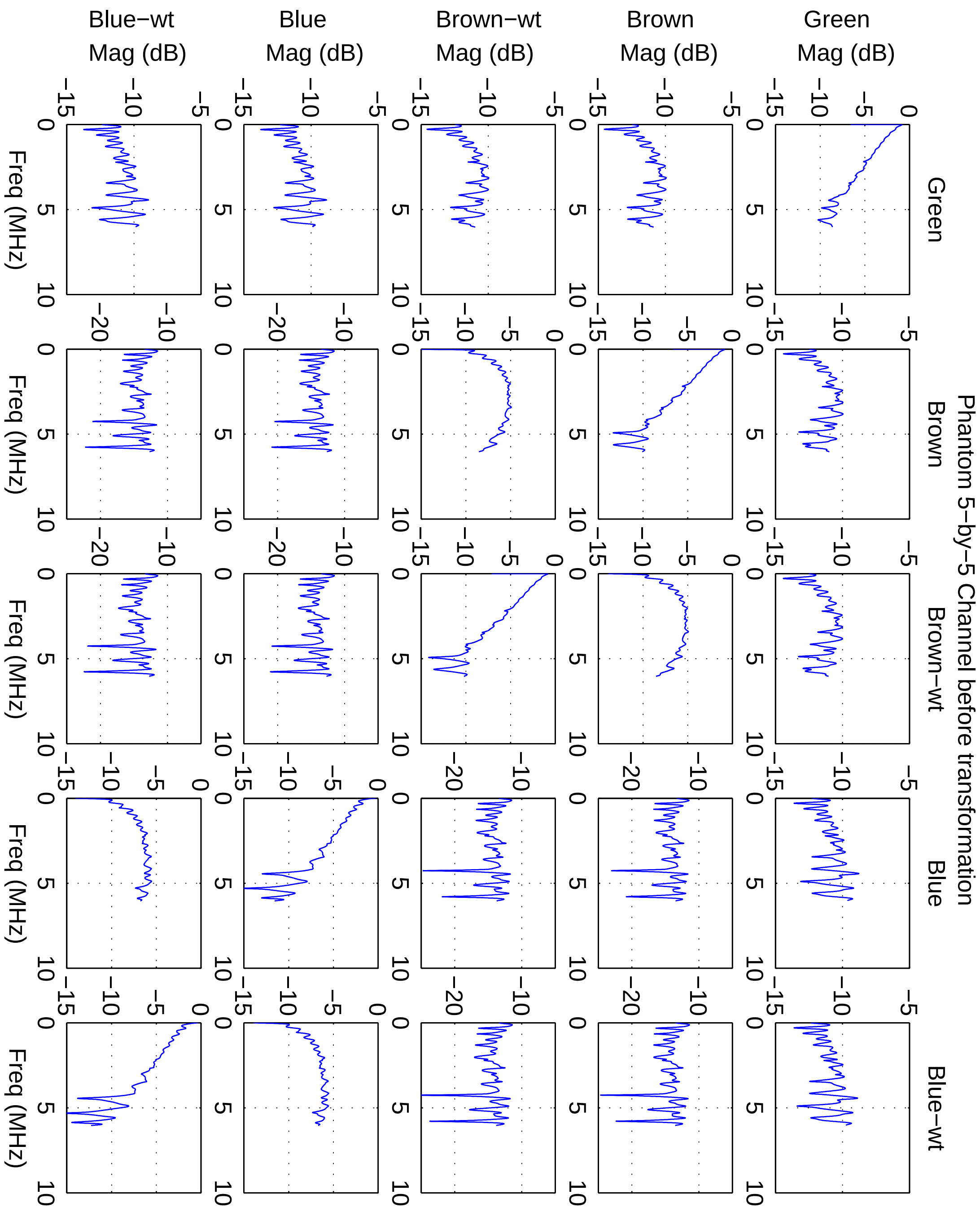

Figure 5.2: Phantom 5×5 Channel before transformation

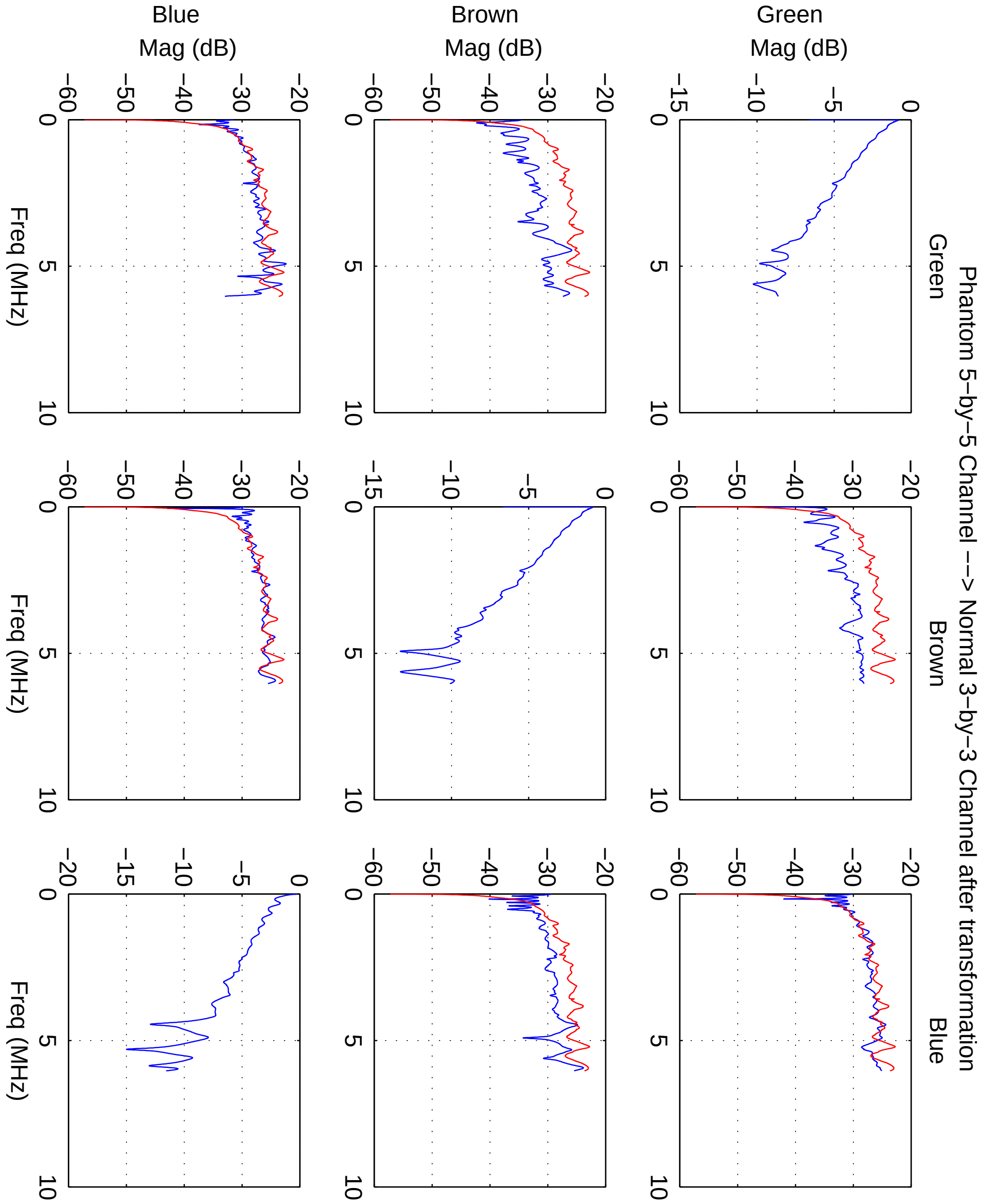

Figure 5.3: Phantom $5 \times 5 \rightarrow$ Normal 3×3 Channel after transformation. Compare the non-diagonal crosstalk elements, normal DSL crosstalk is shown in red while the transformed crosstalk predicted from Phantom 5×5 channel is shown in blue. The diagonal (direct transfer function) remains the same [See equation 5.7 and the discussion there].

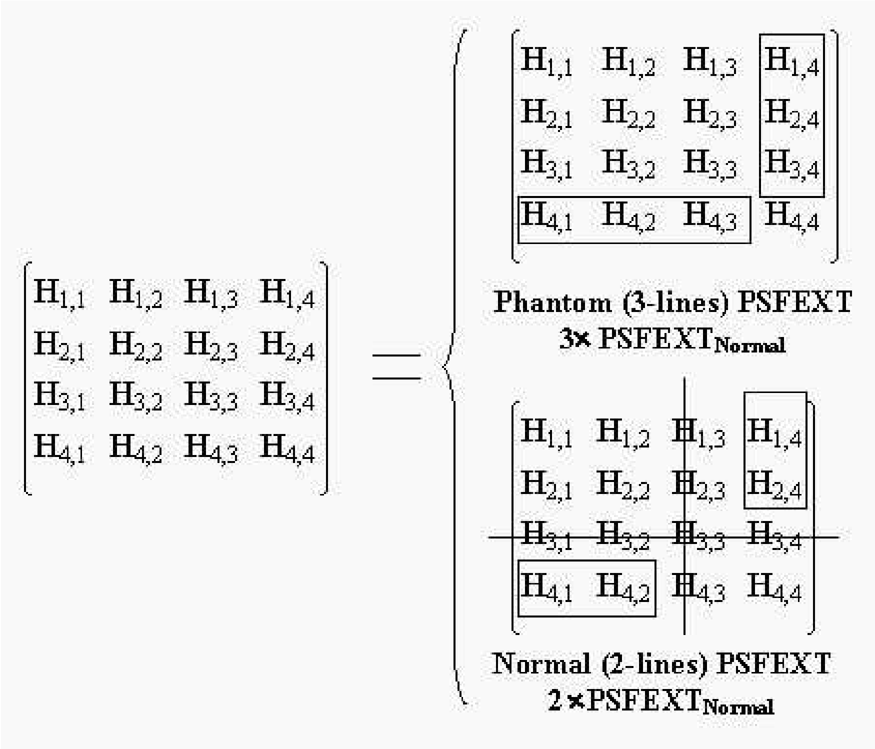

Figure 5.4: Power sum FEXT in simple DSL case and in Phantom channel

3 Phantom wires. Also assume that the crosstalk in the normal mode be $PSFEXT_{Normal}$. The crosstalk as seen on the victim line will therefor be the $3 \times PSFEXT_{Normal}$ for the Phantom mode, while for the same settings in normal mode, i.e. two parallel normal DSL loops, the crosstalk would have been $2 \times PSFEXT_{Normal}$. This is evident from Figure 5.2 where $\mathbf{H_{i,j}} \forall i, j = 1, \ldots, 3$ are used in phantom where $\mathbf{H_{2:3,2:3}}$ is a phantom pair which is used (*a*) in Phantom and (*b*) in normal mode. In normal mode, wire 3 is used as a reference wire and hence eliminated from the normal channel matrix. In all cases wire 4 is considered as the victim line.

This result can further be generalized for n normal DSL loops and a $2n-1$ Phantom DSL. As the number of data channels increases linearly, the power sum crosstalk also increases in the same ratio. Approaches to almost completely mitigate the crosstalk while different normal mode or phantom DSL coexist in the same cable are described in [11], [32] and [30], assuming that the coordination at CO/ONU and therefore a multi-user transmission optimization can be obtained using vectored transmission.

5.3 Summery

Here we provide a relation between Phantom and Normal DSL channel matrices. It is interdicting to see that there is one to one relation exist in these two channels. An intuitive approach is adopted to explain teh phenomena of crosstalk within Phantom and Normal DSL and relate the two with the basic concept of electromagnetic coupling. The crosstalk noise due to the presence of a Phantom DSL in the neighborhood is also discussed and a relation for this is derived.

Future Work and Conclusion

Summery

Summery of the measurement of Phantom Channel characteristics and the capacity comparison are;

1. Phantom channel is defined and identified through measurement.
2. Frequency domain techniques are applied for the channel identification.
3. Phantom channel is compared with normal DSL channel in terms of channel capacity and constraints are mentioned. The comparison are made considering either no crosstalk cancelation is applied or assuming that full crosstalk cancelation is achieved and a comparison is drawn.
4. Gigabit transmission on a DSL using Phantom method is explored.
5. Relation between a phantom and normal DSL channel is established and discussed.
6. Self-crosstalk in a phantom is explored and Power Sum model is suggested.

Conclusions

The study had resulted in the following conclusions,

1. **Crosstalk in Phantom DSL:**
   It was found that crosstalk in Phantom DSL is much higher than its normal DSL counterpart. However, MIMO techniques can be applied to reduce the crosstalk to achieve the data rates close to the channel capacity. The MIMO techniques can either be one side coordination at the CO (see [11], [30]) or two sided coordination (see [32]) depending on the implementation and service in question (short range GDSL or long range Multi-MDSL).

2. **Gigabit on DSL:**

Phantom DSL can provide a data rate of as much as 2.5 Gigabits per seconds on a 4 pair 300 meters loop or 1 Gigabits per seconds on two twisted pairs if the crosstalk is completely mitigated. These data rates on same number of normal DSL channels are not possible and this particular illustration of GDSL describes the tremendous gains of phantom DSL on traditional normal DSL commercially available today, with only one precondition that the crosstalk is properly addressed which is possible through MIMO transmission techniques. High data rates can also be achieved on quads* if similar techniques are applied, however the deployment of quads is constantly discouraged [34].

3. **Phantom vs. Normal DSL Channel:**
   The relation between Phantom and Normal DSL channel is discussed and a relation is established. It was interesting to see how various component in Phantom and Normal DSL channel are correlated. An algorithm is proposed for the same.

4. **Power Sum Crosstalk:**
   It is obvious that the deployment of Phantom DSL can either be in stand alone environments for short to very short lengths (in home DSL, small to moderate sized office premises) or in a bundled environment for long reach. In the first case, crosstalk within the phantom channel can be reduced using various existing fully coordinated MIMO techniques. However, when deployed with other DSL services, crosstalk can be a serious issue to look at. In the later case, Phantom of different dimensions (number of wires used in a phantom channel), together with other DSL variants can exist. At DSL frequencies (depending on if Phantom is used in ADSL range upto 1.104 MHz or in VDSL ranges upto 17.664 MHz), the crosstalk will be a considerable impairments to other services in similar frequency band. PSFEXT model proposed here should give an estimate of the crosstalk generated by phantom DSL present in the vicinity.

5. **Possibilities of Longer Reach:**
   Most of the research in DSL is concentrated on higher data rates at reduced lengths while in the consumer markets, a lot of customers are still untouched with the technology due to the limited reach of existing DSL. IDSL (or ISDN) provides a limited data rates upto 18000Kft. ADSL and VDSL are high data-rate DSL access technology but limited in access area range. Phantom DSL, however, can attain higher data rates at longer DSL lengths if crosstalk can be properly addressed. Same number of wires in Phantom results in almost two times the data channels which can result higher data

*Quad is a 4 wire assembly of wires twisted together. Quads are commonly used in Europe. The crosstalk in Quads is higher than twisted pairs but the crosstalk behavior of all the wires in Quad is more symmetric than in twisted pairs using same number of wires. Also using MIMO techniques a very high data rate could as well be delivered on Quads. This footnote is based on the observation and common crosstalk behaviors of twisted pairs and not studied yet. For more details on Quads please refer to [15]. However note that Quad wires may no longer be used for shorter lengths due to high egress and are generally discouraged.

rates at longer DSL lengths.

However, it is emphasized that more statistical information of the channel should be undertaken for concretely defining the crosstalk terms reached in Section 3.3. A small discussion is provided there emphasizing the need of carrying out extensive experiments to enable the prediction of crosstalk in Phantom DSL.

Future work

The study of Phantom revels that there are still a lot of possibilities left in copper. Phantom DSL in both kind of scenarios, stand alone short and very short lengths and long reach, would lead to better rate and reach then existing DSL (Normal) technologies provided that the crosstalk issues are dealt properly. To this end, few areas for the phantom specific research directions have been identified which should further lay down the new activities in this area. Following are the areas identified,

1. **Phantom DSL: MIMO Crosstalk Cancelation Algorithms:**
   This work has already been identified and being addressed. A report (see [30]) on this is under preparation. This scheme furthers the idea of vectored transmission on tonal set at the CO as described in [10]. It combines the idea of transmitting at singular values of the channel provided that an efficient multi-user decomposition of the channel matrix is possible. **Solving MAC and BC for a Phantom Enabled DSL Access** can be thought as an extension to the MIMO crosstalk cancelation algorithm which will also be studied alongside.

2. **Phantom DSL: MIMO Channel Estimation in Phantom mode**
   DSL channels are relatively stationary and the channel estimation is performed very infrequently (normally at the time of initialization or re-installation). The efficient use of channel depends on the estimated channel transfer function. Error in Channel estimation can lead to the the unappropriate behavior of the channel depending on the robustness of the channel decomposition or transmission techniques with respect to the channel estimation errors.

3. **Effect of Channel Estimation Errors on Crosstalk Mitigation Algorithms**
   An associated (mini)area to look at could be to analyze various MIMO transmission schemes against the channel estimation errors for their robustness.

4. **Phantom DSL: Multiple Nash Equilibria for DSM**
   While Phantom DSL in use, spectrum management can be a tedious task. Phantom

channels themselves should maximize the data rate but unlike their normal DSL counterparts, all Phantom lines will work in tandem to increase the data rate. It is a coordinated scenario within a single Phantom DSL. While deployed along with other services, spectrum management should still be given using multiple Nash equilibrium. This particular situation can be understood as partially coordinated game where players of a team try to maximize their rate while other players, could be of different dimension, (considering number of Phantom lines in a Phantom DSL are the dimension and normal DSL channel can be assumed as a Phantom DSL of dimension one), also try to maximize their data rate. A game theoretic approach can be applied to such a "partially coordinated" multi-user environment. The studies are yet to be made for further investigation.

5. **From** 1 **Gigabits to** 10 **Gigabits**

   It is already shown in 4.4 that gigabit data rates are achievable on a Phantom with 3 or 7 parallel channels. Studies can further be made for the 25 pair cable which can provide as many as 49 parallel phantom channel. The crosstalk in such a case will certainly be very high and highly robust MIMO schemes needed to be presented. Such a possibility can also push the fiber age little further. The 2.5Gbps fiber is still being deployed at several places and the cost involved is already high. A higher data rate on existing copper infrastructure would ensure that the demands of high data rates are satisfied at lower costs.

6. **Long Reach of Phantom DSL**

   From the previous section, if we treat the Phantom channel independently, or assuming full coordination at the CO to apply crosstalk mitigation schemes, it should be possible to achieve considerably higher data rate for longer lengths of DSL loops. More studies in this direction are yet to be made.

7. **Phantom DSL: Proof of Concept Prototype Development**

   Any technology has to be tested in the field, in realistic situations. Recently a master project was done for MIMO wireless communication as a proof of concept. Similar activities can be planned for Phantom DSL in future.

8. **Phantom DSL: Standard Contributions on DSM in Phantom**

   Phantom DSL is a multiline communication scheme with a lot of opportunity for researchers to explore. While exploring various possibilities of Phantom DSL, contribution to the Phantom standards can also be one of the goal.

9. **Concept of Multi-dimensional Multi-user MIMO Techniques**

   As clear from the study of Phantom DSL in a multi-user environment, inherently we also assume that Phantom channel can assume different dimension i.e. number of parallel channels. In the previous case of normal DSL, the multi-user environment assumed to have a single dimension to all of its users. Using Phantom of different dimensions in the same topology, normal DSL channel can be considered as a special case of single dimension with phantom channel assuming any arbitrarily chosen dimension n. This concept gives rise to a multi-dimensional multi-user MIMO environment which poses big challenges. A multi-dimensional multi-user environment can be though as a generalization of existing multi-user environment. Maintaining the integrity of every user within this scenario with users ranging from arbitrary n to a user with only single dimensional. It is proposed to study and solve the concept for the following subclasses as part of this project,

(a) **Multi-dimensional Multi-user MIMO: Solving for Multi-user MAC and BC**
It involves the info-theoretic analysis of multi-dimensional multi-user MIMO environment.

(b) **Multi-dimensional Multi-user MIMO: Wireline Application in Phantom**
Solving the aforementioned general problem wireline applications in Phantom DSL should further be solved.

(c) **Multi-dimensional Multi-user MIMO: Wireless Applications for 4G/5G**
OFDM is already being considered for 4G wireless applications. Introducing multi-dimensional multi-user MIMO environment to wireless application can undoubtedly increase the capacity regions assuming that different number of antenna can be used by a users to increase their bandwidth according to their (business/home) requirements.

The concept of multi-dimensional multi-user MIMO is in its infancy and as part of my studies a proposal will be made for such techniques. Some of the problems in this regard are needed to be addressed further.

Along with this set of tasks, there are a few other areas I would like to make some study and contribute further. These areas could be,

- Wavelets and Multi-tone Modulation Techniques: Feasibility Studies,
- Multi Stage Nash Equilibria: Players Perspective in Coalition of Coalitions
  Game theoretic aspects of a Multi-dimensional Multi-user MIMO environment

Bibliography

[1] Starr T.,Cioffi J.,Silverman P. ”Understanding of DSL”

[2] ”Proposed Requirements for Multi-pair 10MDSL Vectoring” T1E1.4/2003-202 (DSL Access)

[3] DSM Draft Report, T1E1.4/2003-018RA, May 24, 2003, Charlotte, NC.

[4] Jannie Lee Fang, ”Modelling and Characterization of Copper Access Systems”, Ph. D. Dissertation, (with thanks to John Cioffi).

[5] ”Requirements for multi-pair link aggregation for higher rates” - 10MDSL or Enhancements to G.shdsl or Multi-pair link aggregation, T1E1.4/2002-143 (DSL Access)

[6] ETSI Technical Committee Transmission and Multiplexing (TM) Working Group TM6 - ACCESS NETWORKS, ETSI TC TM WG TM6(02)2 April 2002.

[7] ”Proposal for New Work Item in T1E1.4: 10 Mb/s DSL”, T1E1.4/2002-042.

[8] ”IEEE Draft FP802.3ah” EFM task force, April 2004.

[9] ”IEEE 802.3 CSMA/CD Access Method”, IEEE Standards.

[10] G. Ginis and John Cioffi, ”Vectored transmission for digital subscriber loop”, IEEE Journal of Selected Areas in Communication Special Issue on Twisted Pair Transmission, Volume 20, Issue 5, June 2002.

[11] G. Ginis and John Cioffi, ”Vectored-DMT: A FEXT Cancelling Modulation Scheme for Coordinating Users”, Proceedings of IEEE ICC 2001, Vol 1, Helsinki, Finald, pp 305-309, June 2001

[12] ”www.ieee802.org/3/efm/public”, Ethernet in First Mile, IEEE 802.3ah, EFM-task force.

[13] J. Helszajn, ”Passive and Active Microwave Circuits”, John Wiley & Sons, 1978.

[14] Pozar D. M., ”Microwave Engineering”, Addison-Wesley Publishing Co., 1998.

[15] Skilling, Hugh Hildreth, ”Electric transmission lines: distributed constants, theory and applications”, McGraw-Hill New York (N.Y.), 1951.

[16] Lao R., ”The twisted-pair telephone transmission line”, High Frequency Design, November 2002.

[17] Measurement Laboratory - ESAMAT, Microelectronics and Sensors (MICAS), ESAT, KU Leuven, Heverlee-Leuven, Belgium.

[18] RF-Laboratory, Interuniversity MicroElectronics Center (IMEC), Kapeldreef-74, Heverlee-Leuven, Belgium.

[19] S Galli, C Valenti, K. J. Kerpez, ”A frequency -domain approach to crosstalk identification in xDSL systems”, IEEE journal on Selected Areas in Communications, August 2001

[20] R. Pintelon, P. Guillaume, Y. Rolain, J. Schoukens, and H. Vanhamme, ”Parametric Identification of Transfer Functions in the Frequency Domain - A Survey”, IEEE Transection of Automatic Control, Vol 39, pp 2245-2260, 1994.

[21] Levy E. C., ”Complex Curve Fitting”, IRE Transection on Automatic Control, vol. AC-4, pp 37-43, 1959.

[22] Sanathanan C. K. and J. Koerner, ”Transfer function synthesis as a ratio of two complex polynomals”, IEEE Transection on Automatic Control, vol. AC-8, pp 56-58, 1963.

[23] B. Farhang-Boroujeny, ”Adaptive Filters: Theory and Applications”, John Wiley & Sons, Chichester, England, 1998.

[24] George E. Forsythe, ”Generation and Use of Orthogonal Polynomials for Data-Fitting with a Digital Computer”, J. SIAM, Vol 5, pp 74-88, 1957.

[25] Kelly Louis G., ”Handbook of Numerical Methods and Applications”, Addison-Wesley Publishing Co, 1967.

[26] P.S.C. Heuberger, O.H. Bosgra and P.M.J. Van den Hof, ”A Generalized orthonormal basis for linear dynamical systems,” IEEE Transection Automation and Control, vol 40, pp. 451-465, 1994.

[27] Schoukens J, Pintelon R., ”Identification of Linear Systems”, 1991.

[28] Ljung L., ”Some Results on Identifying Linear Systems using Frequency Domain Data” in Proc. 32nd IEEE Conference on Decision Control, San Antonio, TX, pp. 3534-3538, 1993.

[29] Ljung L., ”System Identification: Theory for the user,” Englewood Cliffs, NJ, Prentice-Hall, 1987.

[30] Narendra Kumar Saini, Marc Moonen, ”Per-tone crosstalk cancellation Scheme for Digital Subscriber-Line Network”, *In preparation*.

[31] ”www.dslprime.com”, in a presentation in March 2004.

[32] Georg Taubock, Werner Henkel, ”MIMO Systems in the Subscriber-Line Network”, 5th Internationa OFDM-Workshop, Hamburg, 2000.

[33] ”Spectrum Management for Loop Transmission Systems”, ANSI Standard T1.417-2001, NY.

[34] ”Commercial Building Telecommunications Cabling Standard”, TIA/EIA-568A.

[35] ”Transmission and Multiplexing (TM): Access transmission systems on metallic access cables, VDSL Functional Requirements”, ETSI Std. TS 101 270-1, Rev. V.1.3.1, 2003.